BOUT++ Physics development

Presented to 2015 BOUT++ mini-Workshop

Xueqiao Xu
and BOUT++ team

Dec 16-18, 2015, Livermore, California

LLNL-PRES-680206
This work was performed under the auspices of the U.S. Department of Energy by Lawrence Livermore National Laboratory under contract DE-AC52-07NA27344. Lawrence Livermore National Security, LLC

Lawrence Livermore National Laboratory

ACKNOWLEDGMENTS

The author would like to acknowledge significant contributions to this presentation from following collaborators:

B. Cohen, J. G. Chen, A. Diallo, A. Dimits, B. Dudson, P. H. Diamond, M. E. Fenstermacher, X. Gao, R. Groebner, Ted Golfinopoulos, C. Holland, A. E. Hubbard, J.W. Hughes, I. Joseph, Z.X. Liu, M. Kim, S. S. Kim, D. F. Kong, G. Q. Li, C. H. Ma, J. F. Ma, B. H. Meyer, P. B. Snyder, T. F. Tang, M. V. Umansky, H. Wilson, Z. H. Wang, P. W. Xi, T. Y. Xia, G. S. Xu, and N. Yan.

Tokamak edge region encompasses boundary layer between hot core plasma and material walls

- Complex geometry
- Rich physics (plasma, atomic, material)

- Sets key engineering constraints for fusion reactor
- Sets global energy confinement

Tokamak interior

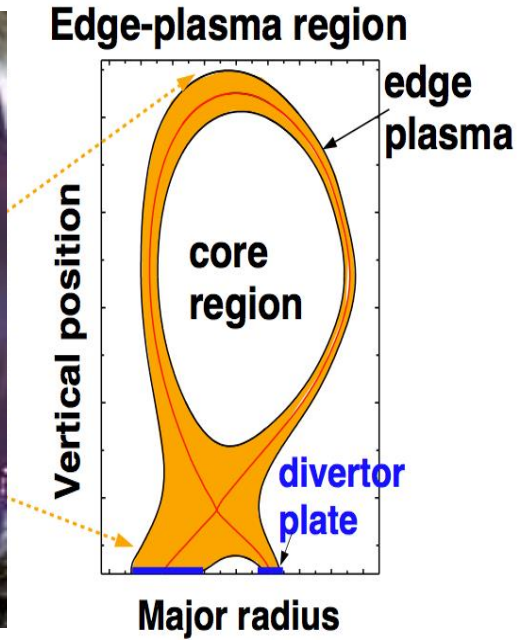

BOUT (BOUndary Turbulence) was originally developed at LLNL in late 1990s for modeling tokamak edge turbulence

BOUT++ is a successor to BOUT, developed in collaboration with Univ. York

Original BOUT, tokamak applications on boundary turbulence and ELMs with encouraging results

BOUT++
Boundary Plasma Turbulence Code

BOUT-06: code refactoring using differential operator approach, high order FD, verification

BOUT++: OOP, 2D parallelization, applications to tokamak ELMs and linear plasmas

- ✓Gyro-fluid extension
- ✓RMPs & RF
- ✓Neutrals & impurities
- ✓Preconditioner
- ✓Validation

2000 2005 2015

- *X.Q. Xu and R.H. Cohen, Contrib. Plasma Phys. 38, 158 (1998)*
- *Xu, Umansky, Dudson & Snyder, CiCP, V. 4, 949-979 (2008).*
- Umansky, Xu, Dudson, et al., , Comp. Phys. Comm. V. *180 , 887-903 (2008).*
- Dudson, Umansky, Xu et al., Comp. Phys. Comm. V.180 (2009) 1467.
- Xu, Dudson, Snyder et al., PRL 105, 175005 (2010).

Principal BOUT++ Activities

- A suite of two-fluid multiple-field models has been implemented in BOUT++ for
  - ✓ all ELM regimes and fluid turbulence

    T. Y. Xia, 3rd talk this afternoon

- A suite of 3+1 Gyro-Landau-Fluid models is also developed for
  - ✓ pedestal kinetic turbulence and transport

    C.H. Ma, 2nd talk this afternoon

- Fluid neutral models are developed for
  - ✓ SMBI, GAS puffing, Recycling

- A PIC module for impurity generation and transport

- Coupling BOUT++ and SOLPS for divertor heat flux contr.

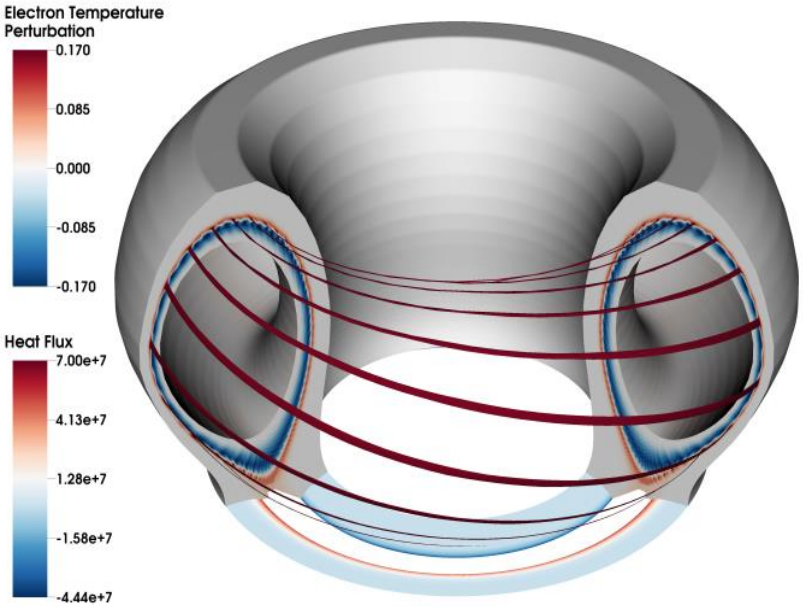

- BOUT++ has been applied to a range of problems, including simulation of ELMs, plasma blobs, turbulence, & magnetic reconnection

Benchmarks

(module elm_pb)

BOUT++ 3-field reduce MHD model (module elm_pb)

- **3-field reduced MHD equations evolve pressure P, vorticity ϖ and perturbed magnetic vector potential $A_\parallel$:**

$$\frac{\partial \tilde{\varpi}}{\partial t} + v_E \cdot \nabla \tilde{\varpi} = B_0 \nabla_\parallel \tilde{J}_\parallel + 2 b_0 \times k_0 \cdot \nabla \tilde{P}$$

$$\frac{\partial P}{\partial t} + v_E \cdot \nabla P = 0$$

$$\frac{\partial \tilde{A}_\parallel}{\partial t} = -\nabla_\parallel \Phi + \frac{\eta}{\mu_0} \nabla_\perp^2 \tilde{A}_\parallel$$

- **The variables in the equations are defined as:**

$$\tilde{\varpi} = \frac{n_0 M_i}{B_0}\left(\nabla_\perp^2 \tilde{\phi} + \frac{1}{n_0 Z_i e} \nabla_\perp^2 \tilde{P}\right), \Phi = \tilde{\phi} + \Phi_0, k_0 = b_0 \cdot \nabla b_0$$

$$J_\parallel = J_{\parallel 0} - \frac{1}{\mu_0} \nabla_\perp^2 \tilde{A}_\parallel, \qquad v_E = \frac{1}{B_0}(b_0 \times \nabla_\perp \Phi)$$

- **In the equations, for any variable *F*, $\tilde{F}$ is the perturbed component,**
$\nabla_\parallel F = B \partial_\parallel (F/B)$, $\partial_\parallel = \partial_\parallel^0 + b \cdot \nabla$, $b = B/B = \nabla_\parallel A_\parallel \times b_0/B$, $\partial_\parallel^0 = b_0 \cdot \nabla$

JET-like Equilibrium model

- **Based on the cbm18 equilibrium sequence**
- **Circular plasma, with a "vacuum" region**
- **BOUT++ computation region is ψ [0.2, 1.4]**

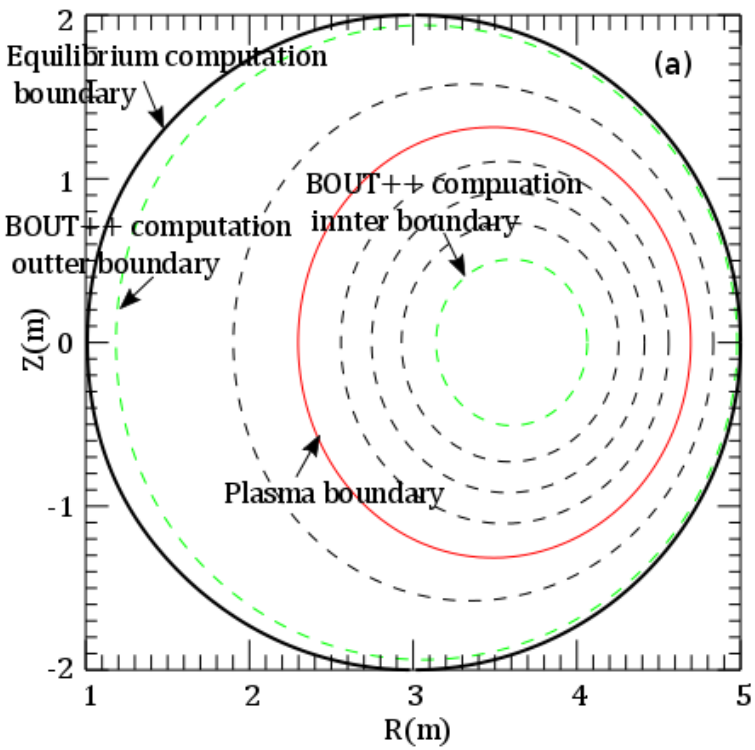

Plasma configuration

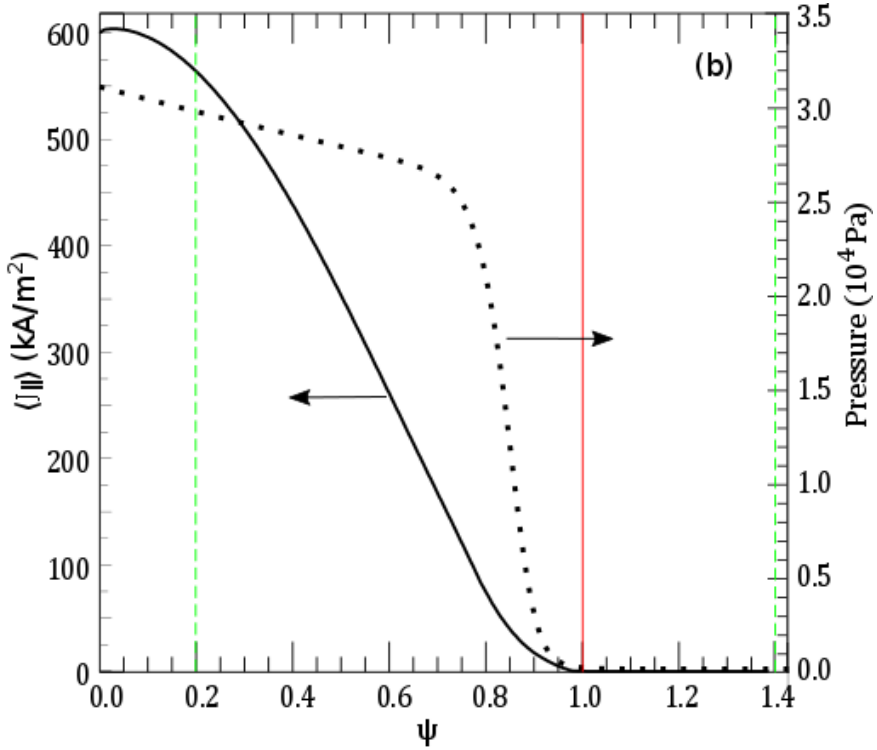

Current and pressure profiles

A set of JET-like equilibria with different edge current

- **Based on the cbm18_dens8 equilibrium, using the CORSICA code, a sequence of equilibrium with different edge current are created**
- **Keep total current and pressure profile fixed**

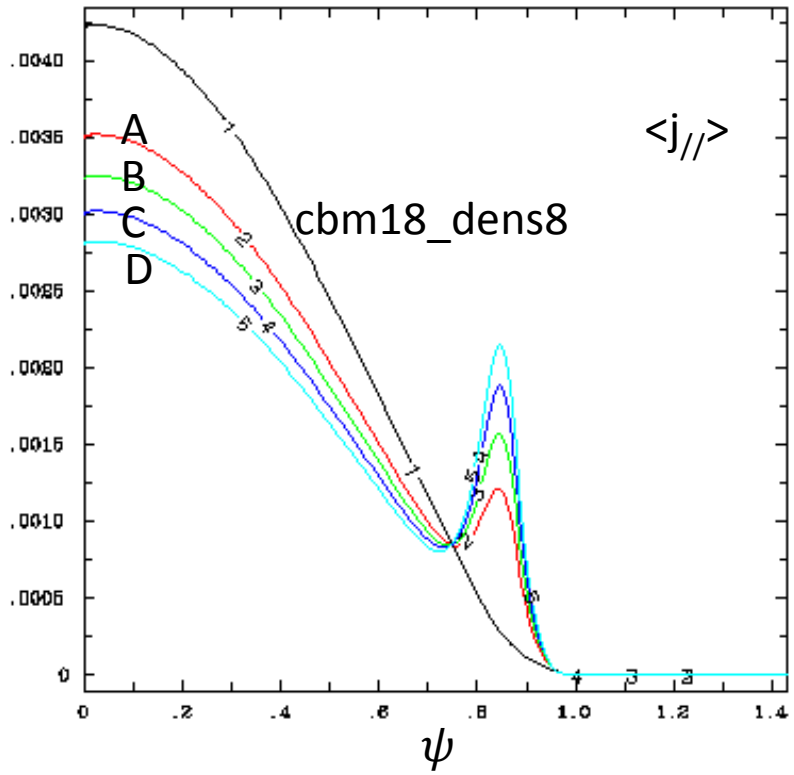

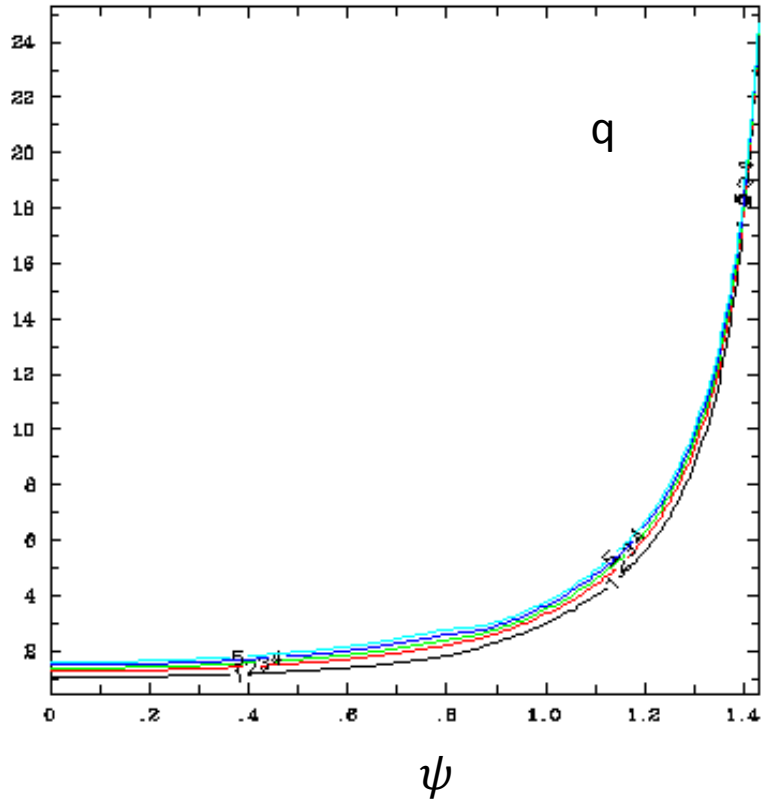

Edge current has stabilizing effects on the ballooning modes

- **As the edge current increases, the medium n ballooning modes are stabilized, the dominant mode is changed from ballooning modes to low-n kink modes**
- **The ballooning stabilization effect is due to the increase of local shear at the outer mid-plane**

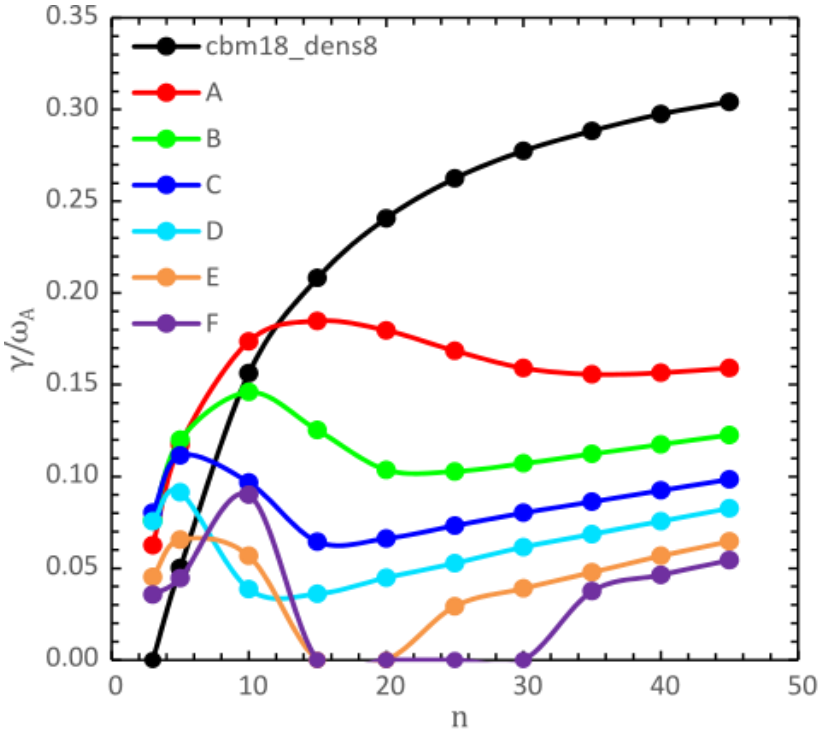

Linear growth rate v.s. toroidal mode number

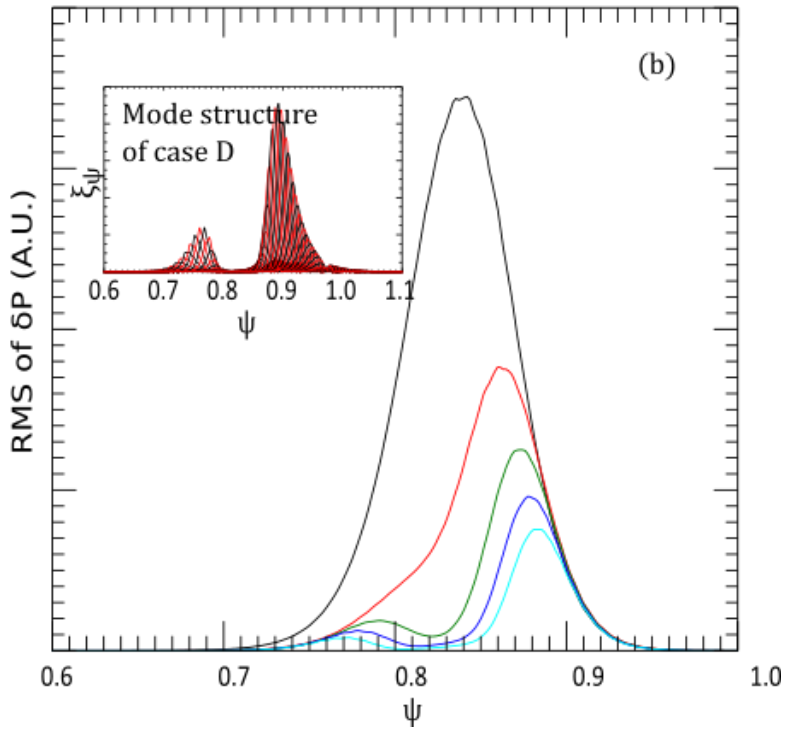

RMS of perturbed pressure, the height is normalized with linear growth rate

Good agreement between BOUT++, ELITE and GATO for both peeling and ballooning modes

- **As edge current increases, the difference between BOUT++ and GATO/ELITE results becomes large**
- **This difference is due to the vacuum treatment**

For the real "vacuum" model, the effect of resistivity should be included as BOUT++

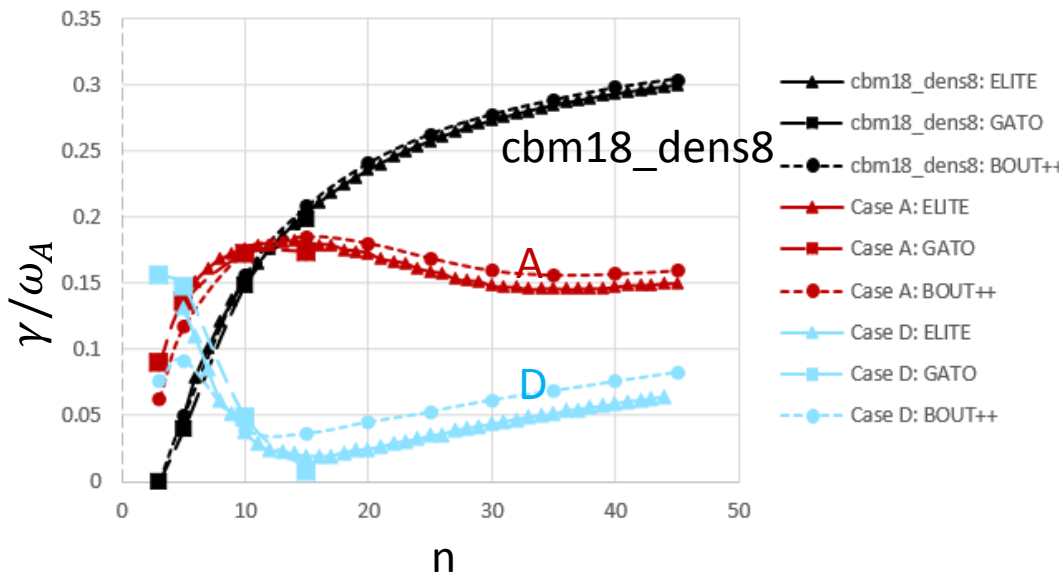

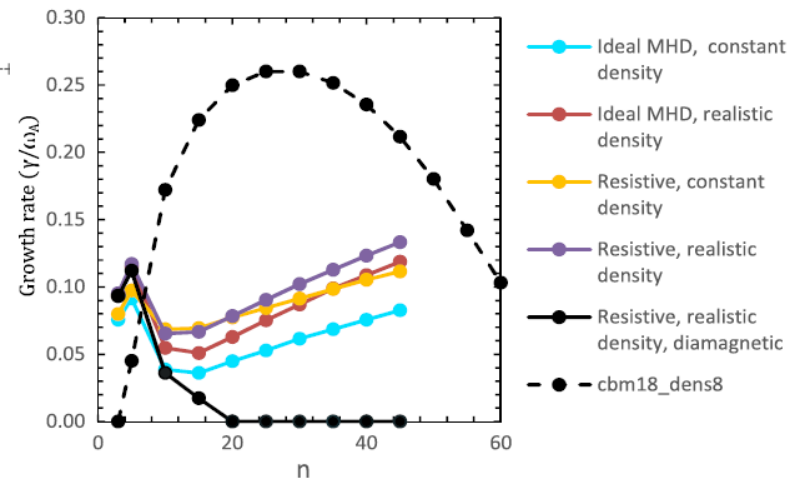

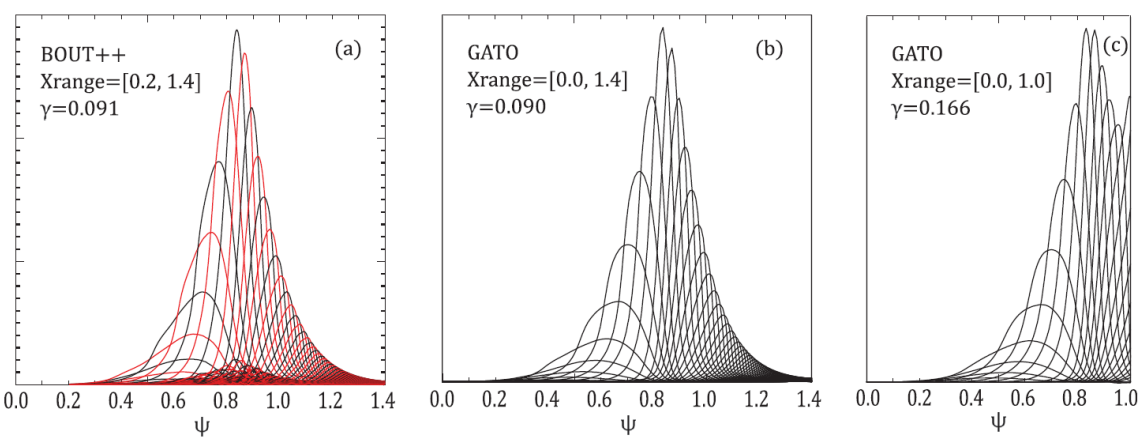

G. Q. Li, X. Q. Xu, P. B. Snyder, A. D. Turnbull, T. Y. Xia, C. H. Ma and P. W. Xi, *Phys. Plasmas* 21, 102511 (2014)

Benchmark results for elongated plasma for both peeling and ballooning modes

- **Elongated dbm18 equilibrium**
  - **Elong=1.32, R0=3m, Ip=2.25MA, Bt0=2.0T, betaN=1.68**
- **BOUT++ agrees with GATO if they use same vacuum model**
- **Vacuum model has small effects on the stability, though it is the ballooning dominated mode**

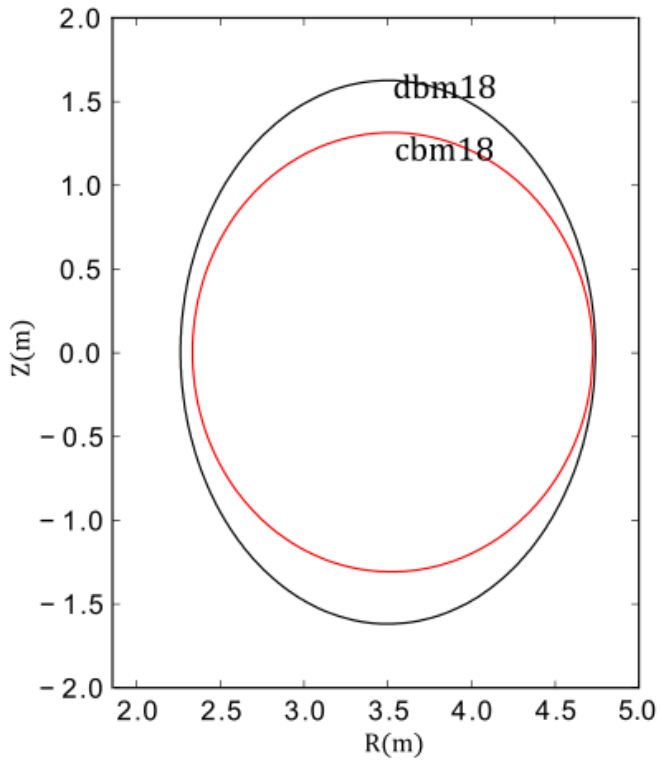

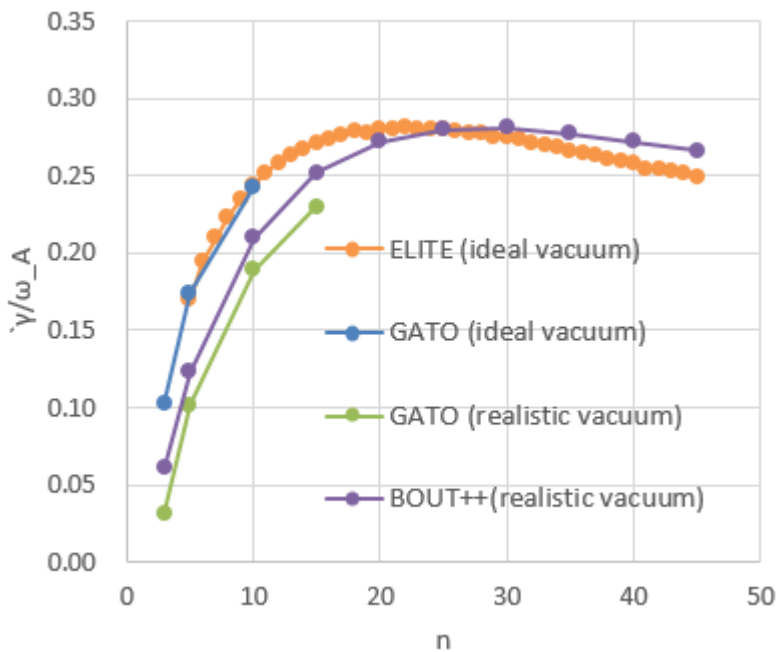

G. Q. Li

Nonlinear ELM simulations show three stages of an ELM event

- **BOUT++ 3-field reduce MHD model evolves**
  - ✓ **pressure P**
  - ✓ **vorticity ϖ**
  - ✓ **magnetic vector potential $A_{\parallel}$**

- **Based on a set of JET-like magnetic equilibria**
  - ✓ **Circular plasma, with a "SOL" region**
  - ✓ **BOUT++ computation region in ψ [0.1, 1.4]**

ELM: Edge-localized Modes

MAST

A Kirk

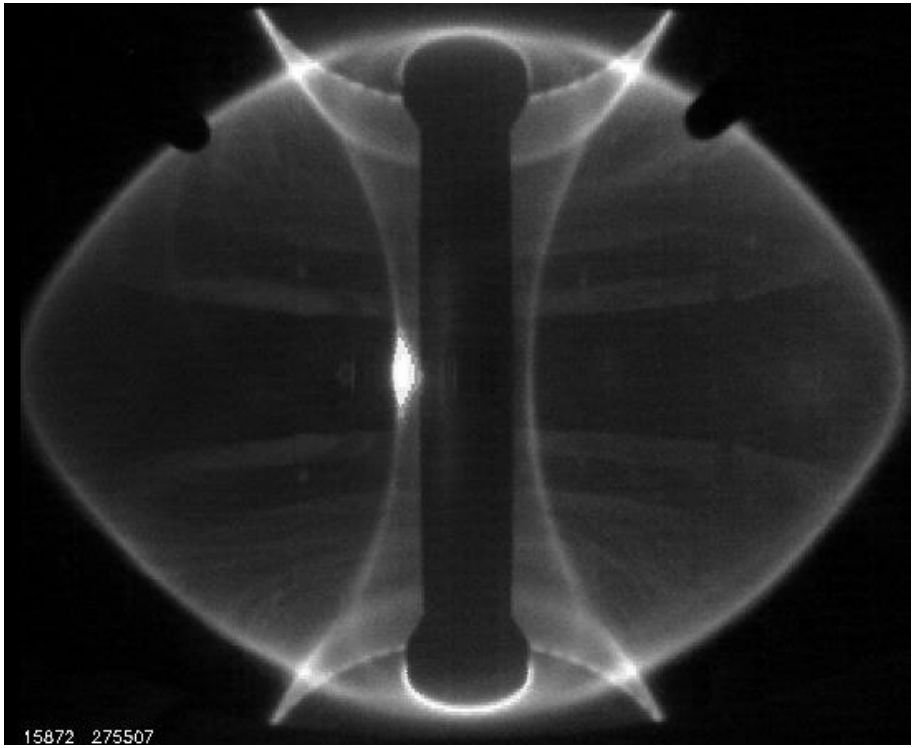

DIII-D

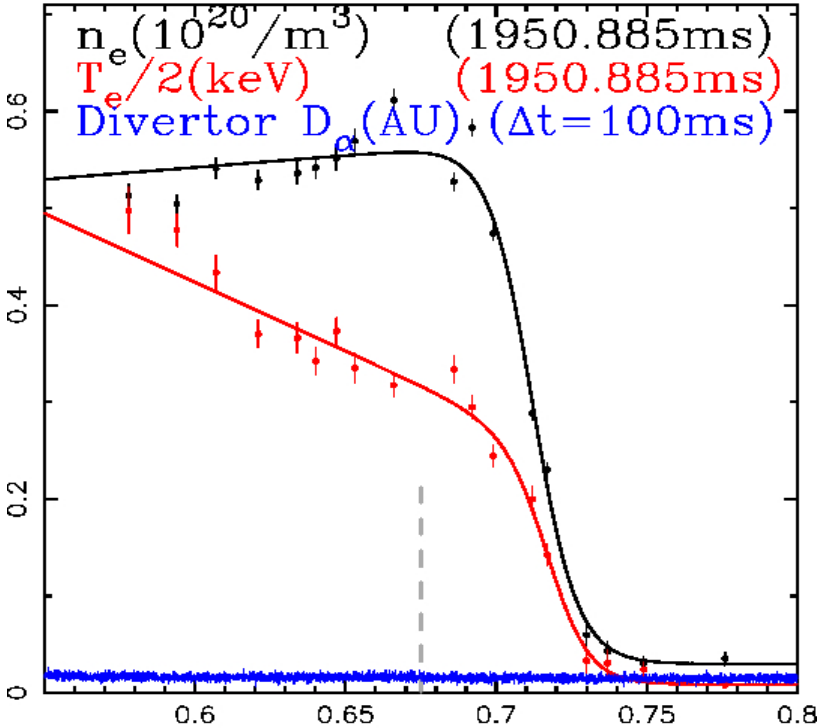

DIII-D Pedestal Region: Z(m)

- **The ELMs are quasiperiodic relaxations of the pedestal, resulting in a series of hot plasma eruptions**
  - ✓ **Potentially damage the ITER divertor plates and first walls**

A. W. Leonard, APS review talk (2013); Phys. Plasmas 21, 090501 (2014)

ELM: Edge-localized Modes

MAST A Kirk

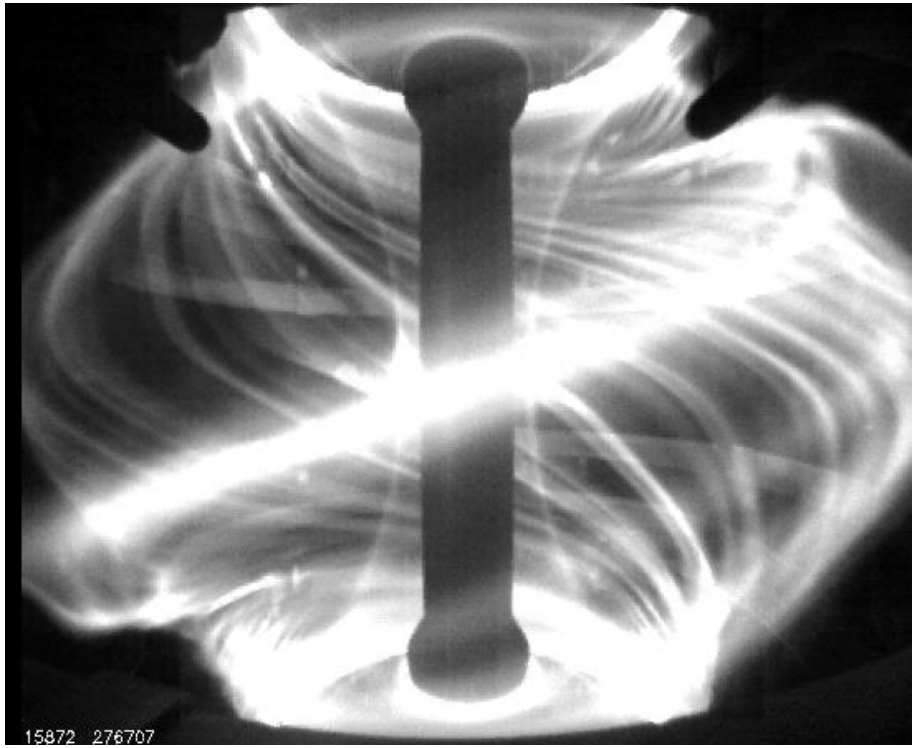

DIII-D

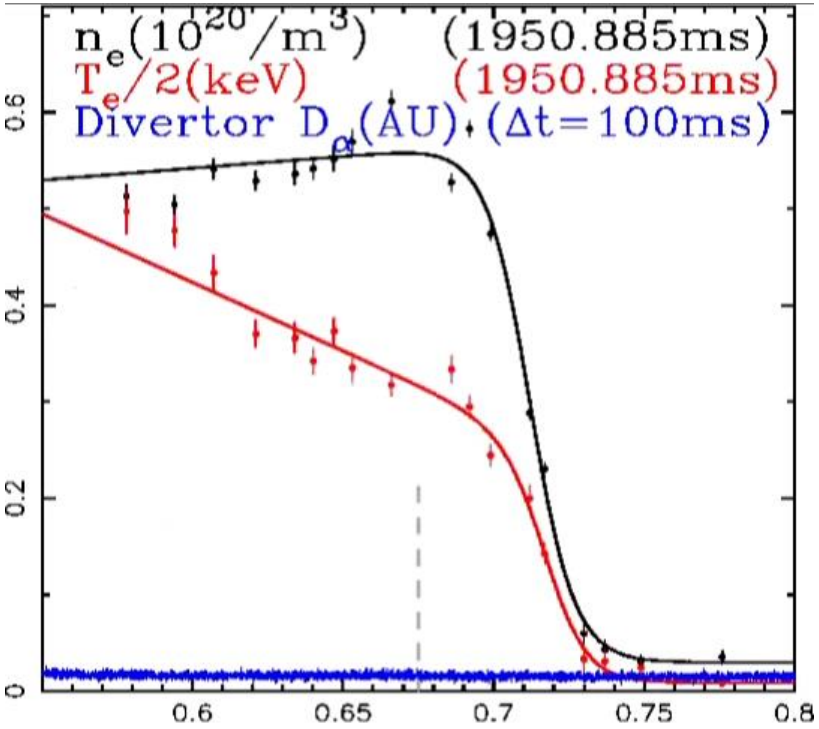

DIII-D Pedestal Region: Z(m)

- **The ELMs are quasiperiodic relaxations of the pedestal, resulting in a series of hot plasma eruptions**
  - ✓ **Potentially damage the ITER divertor plates and first walls**

A. W. Leonard, APS review talk (2013); Phys. Plasmas 21, 090501 (2014)

Principal Results

- **Demonstrated the linear and nonlinear characteristics of ELMs at different collisionality & Er via a density scan**

- **By increasing collisionality, nonlinear simulations show that**
  - ✓ **Power spectrum becomes broad, the dominant mode increases from n=6 to n=35**
  - ✓ **Bispectrum analysis shows that nonlinear mode coupling becomes stronger, resulting in the lack of dominant filamentary structures and reduced ELM energy loss.**

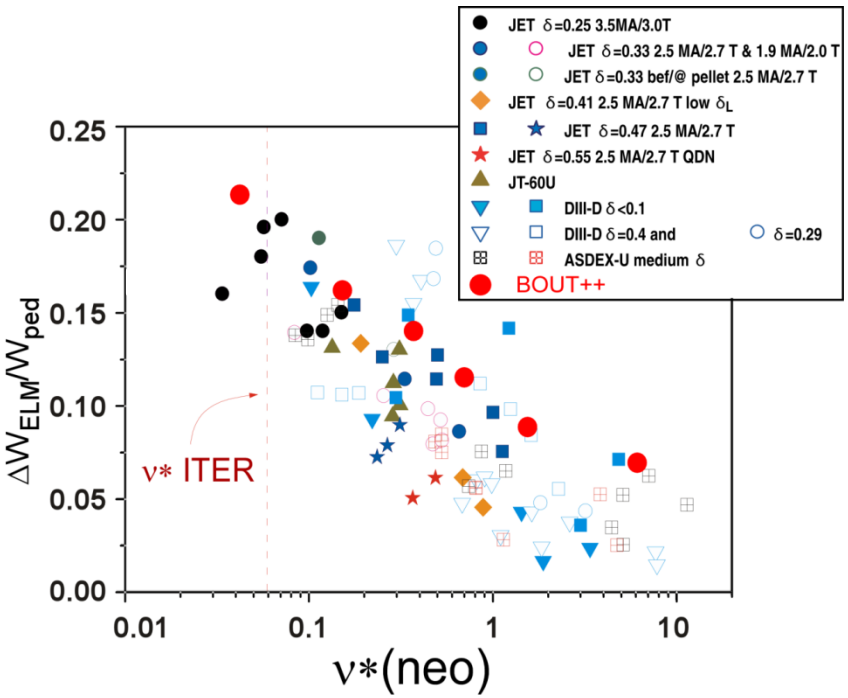

- **The impact of radial electric field Er on peeling and ballooning modes is different.**
  - ✓ **The increase Er significantly enhances the linear growth rate of low-n peeling modes, but only weakly impacts on nonlinear ELM energy loss**
  - ✓ **The increase Er leads to large suppression of nonlinear ballooning amplitudes, but only weakly impacts on their linear growth rates.**

We create a set of equilibria with the self-consistent variation of density and temperature profiles, while keeping the plasma cross-sectional shape, total stored energy, total plasma current and pressure profile fixed.

- Eight cases: $n_e(0)$=1, 3, 5, 7, 9, 12, 15, 20x10^{19} m^{-3}.
- $n_e = n_e(0) * \left(\frac{P0}{P0(0)}\right)^{0.3}$, $T_e = \frac{P0}{2n_e}$.

$$\mathbf{V}_{\perp 0} = \frac{1}{Zen_{i0}} \frac{\mathbf{b} \times \nabla P_{i0}}{B} + \frac{\mathbf{b} \times \nabla \Phi_{dia0}}{B}$$

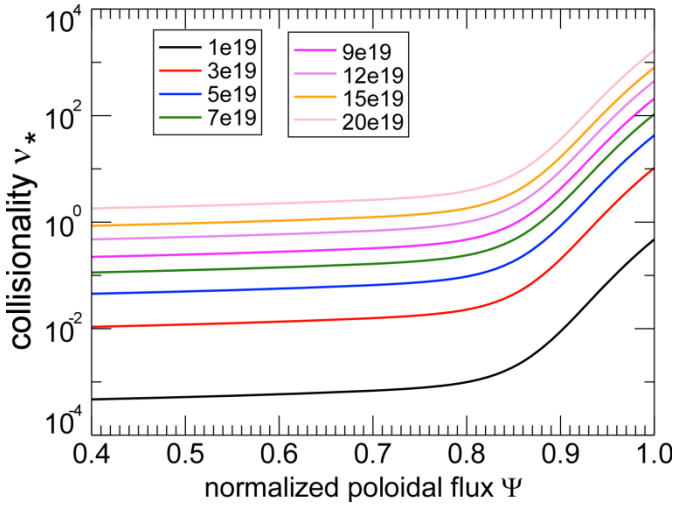

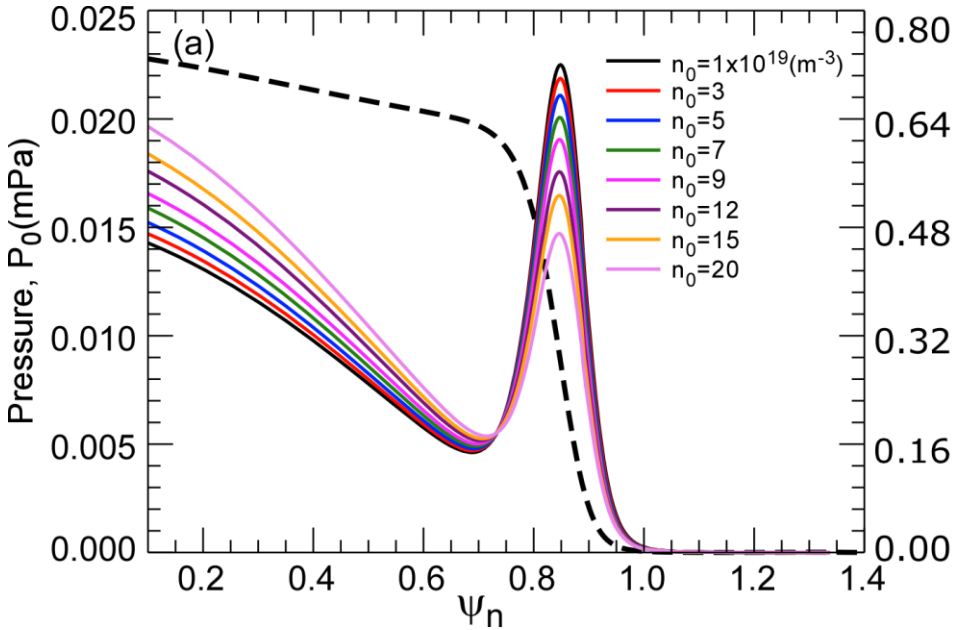

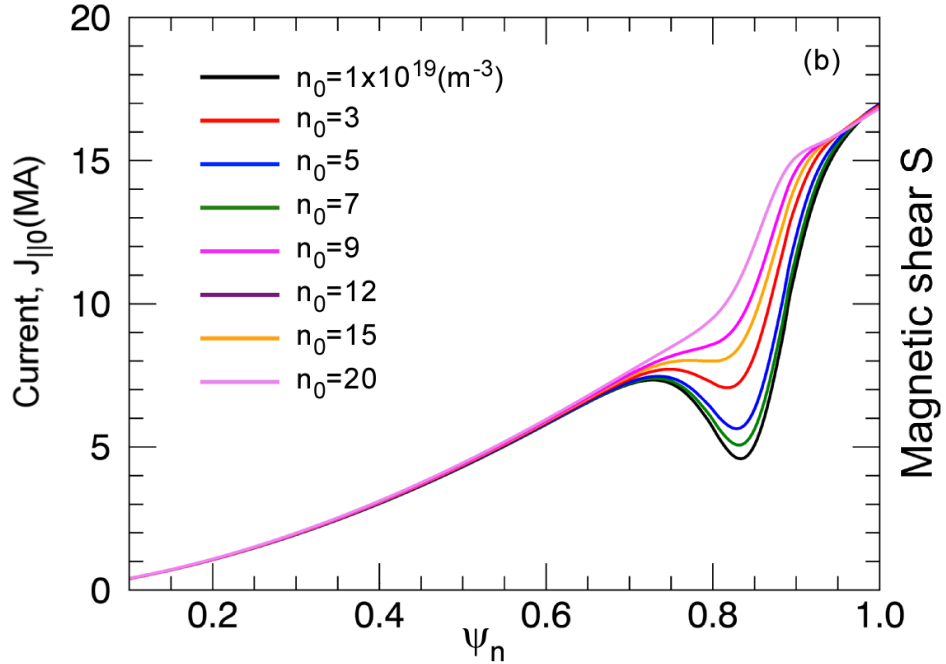

Nonlinear ELM simulations show three stages of an ELM event

1) a linear growth phase
2) a fast crash phase
3) a slow inward spreading phase
   - In 3-field 2-fluid model, total energy loss (P) shows a similar spreading
   - In 3+1 GLF model, Electron perturbation provides the spreading, eventually dominates the total energy loss with a large conductive energy loss

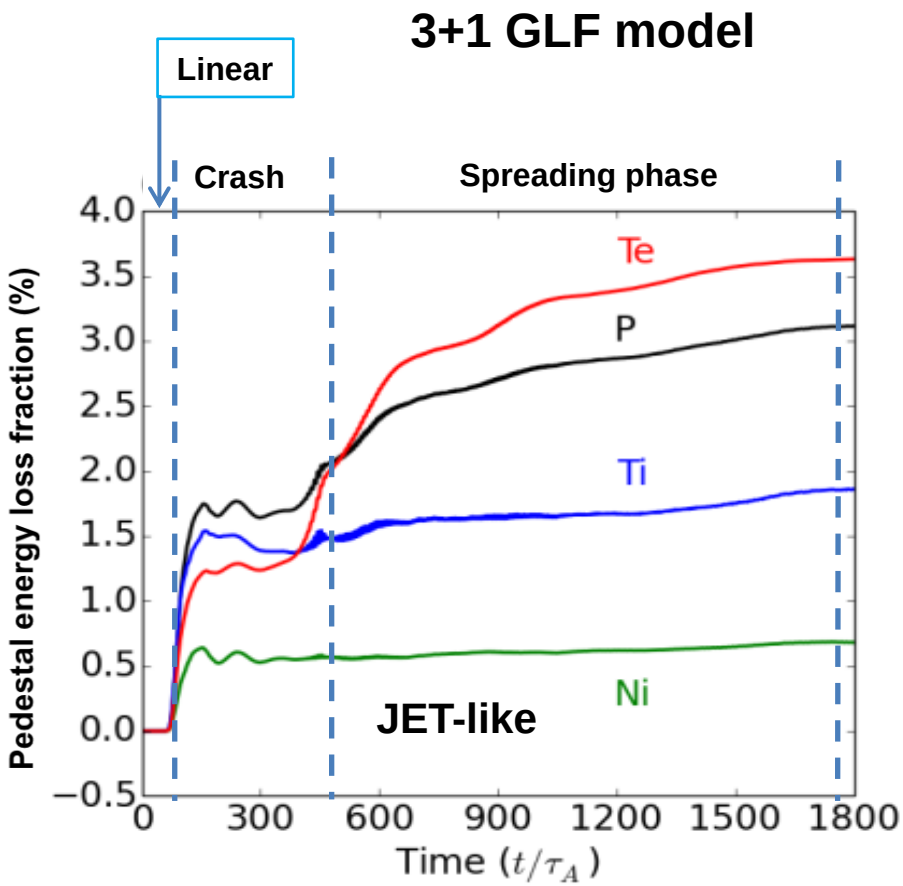

C. H. Ma, et al. Phys. Plasmas 22, 010702 (2015)

As the edge density (collisionality) increases for fixed Er, the growth rate of the P-B mode increases for high n but decreases for low n (1<n<5)

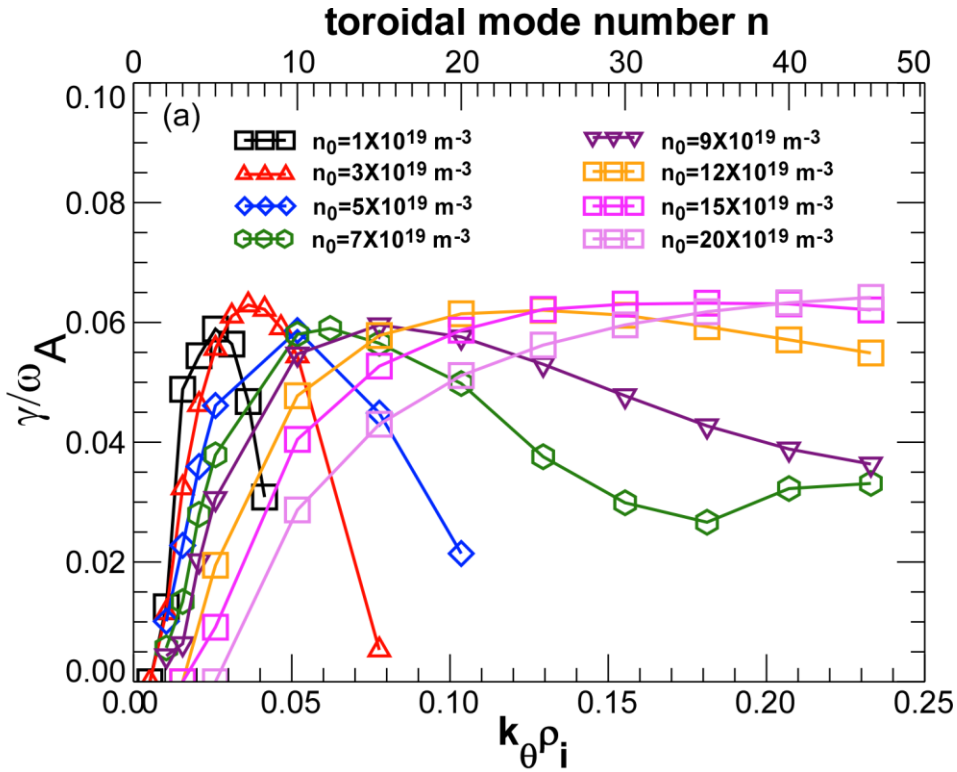

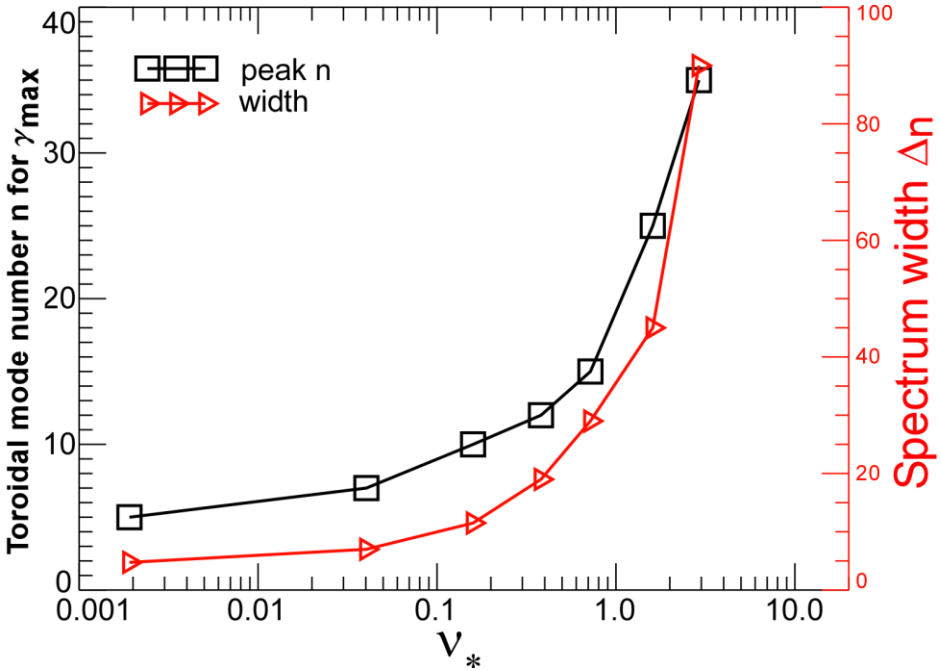

- The ballooning term dominates the high n modes. Because ion diamagnetic drift is inversely proportional to the density for fixed pressure, when density increases, the ion diamagnetic stabilization decreases and growth rate increases.

- The kink term dominates the low n modes. Therefore, as the density increases, the edge current decreases and growth rate decreases.

The growth time of linear drive is determined by nonlinear process via phase evolution for large ELM crash

ELM crash

Linear drive

$$\exp(\gamma t) \leftarrow \begin{cases} \gamma \\ t \end{cases}$$

Pressure gradient (Ballooning mode)

$$2\mathbf{b}_0 \times \boldsymbol{\kappa} \cdot \nabla \tilde{P}$$

Dominant

Large amplitude

$$A_{n\neq 0}$$

Weak

Nonlinear wave-wave interaction (C_R)

Relative phase

$$\delta\varphi(n,\psi,\theta,t) = \arg\left(\frac{\hat{P}_n(\psi,\theta,t)}{\hat{\phi}_n(\psi,\theta,t)}\right)$$

ELM size vs nonlinearity C_R

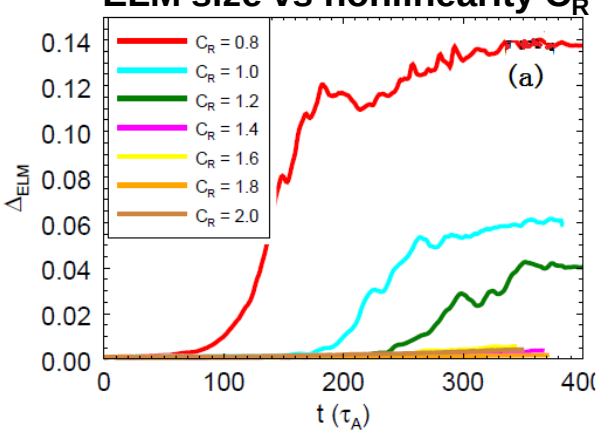

PCT vs nonlinearity C_R

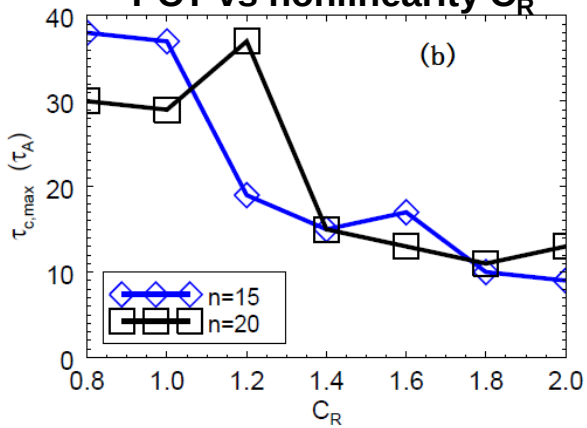

$$\frac{\partial \varpi}{\partial t} + C_R \frac{\mathbf{b} \times \nabla \phi}{B} \cdot \nabla \varpi = RHS$$

Phase coherence time (PCT, τ_c): the length of time duration of the **relative phase** for linear growth

→Linear theory/simulations: unchanged $\delta\varphi \Rightarrow \tau_c \to \infty$

→The growth time is determined by nonlinear Phase Scattering

Xi, Xu, Diamond, Phys. Plasmas 21, 056110 (2014)

2D bispectrum shows that nonlinear mode coupling becomes stronger at high collisionality ν*

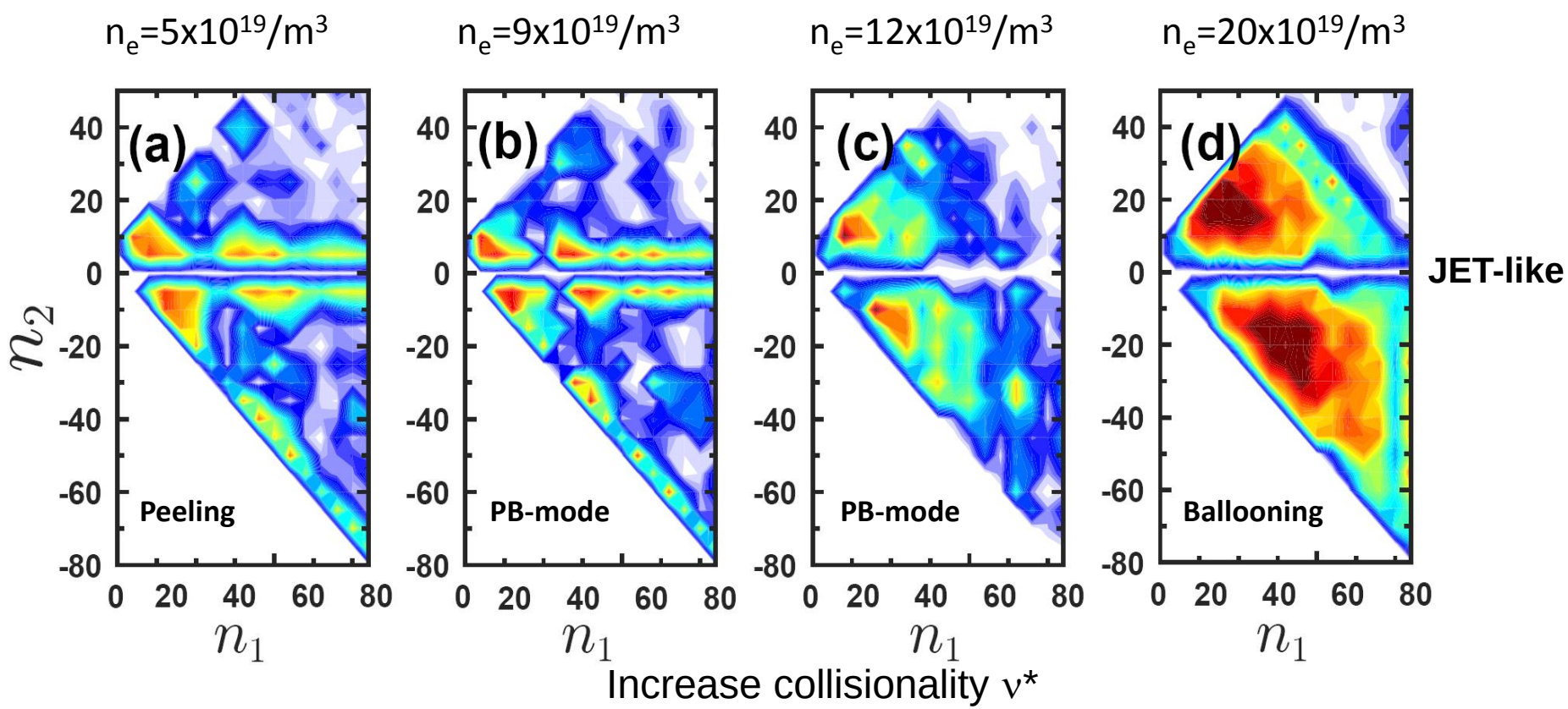

Stronger nonlinear mode coupling at high ν* leads to the lack of dominant filamentary structures and the reduced ELM energy loss.

BOUT++ simulations show collisionality scaling of ELM energy losses consistent with ITPA multi-tokamak database

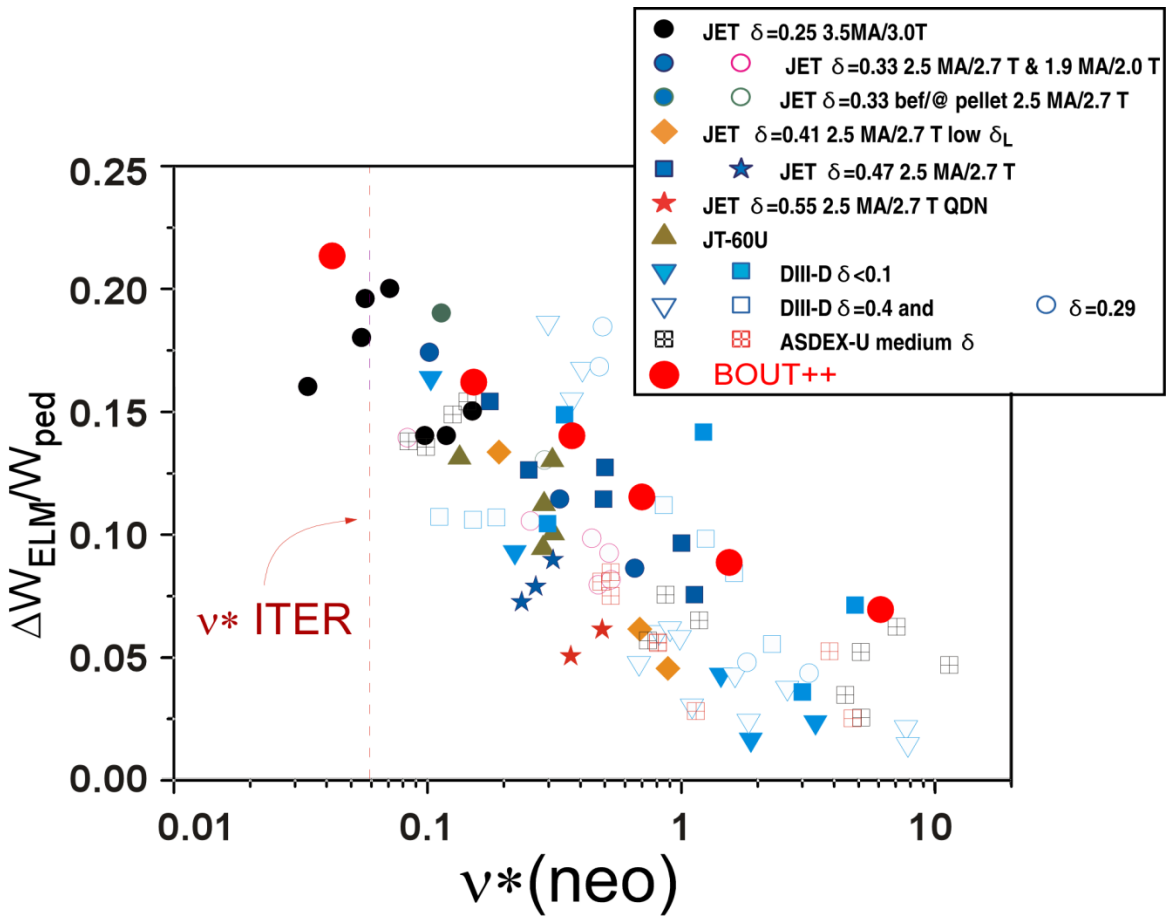

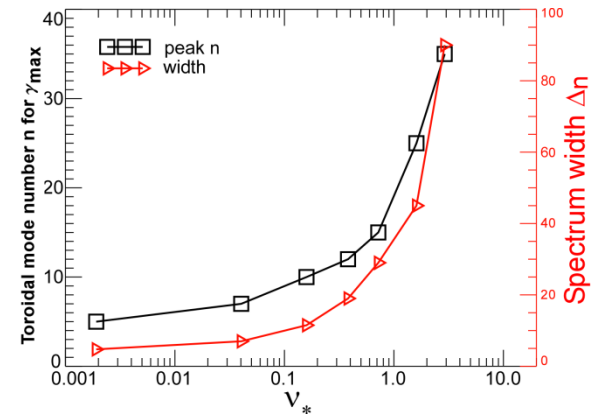

Two factors determine if a single mode amplitude can grow to a large magnitude to trigger an ELM

- **Linear growth rate**
- **Nonlinear growth time**

$$\exp(\gamma t) \leftarrow \begin{cases} \gamma < -\text{linear} \\ t < -\text{nonlinear} \end{cases}$$

As the edge collisionality decreases, both linear and nonlinear physics set ELM energy loss

- **Linearly, the dominant P-B mode shifts to lower n and the spectrum width of the linear growth rate decreases**
- **Nonlinearly,**

  Narrow mode spectrum → Weak nonlinear Phase Scattering →Long PCT →Large ELMs

Equilibrium electric field model

$$\mathbf{V}_{\perp 0} = \frac{1}{Zen_{i0}} \frac{\mathbf{b} \times \nabla P_{i0}}{B} + \frac{\mathbf{b} \times \nabla \Phi_{dia0}}{B}$$

$$\hat{\Phi}_{dia0} = -\frac{\bar{B}}{1.4\mu_0 ZeV_A \bar{L} N \hat{n}_{i0}} \frac{\hat{P}_{00}^{0.3} \hat{P}_0^{0.7}}{\hat{B}_0}$$

Evolution of electric field during ELM crashes

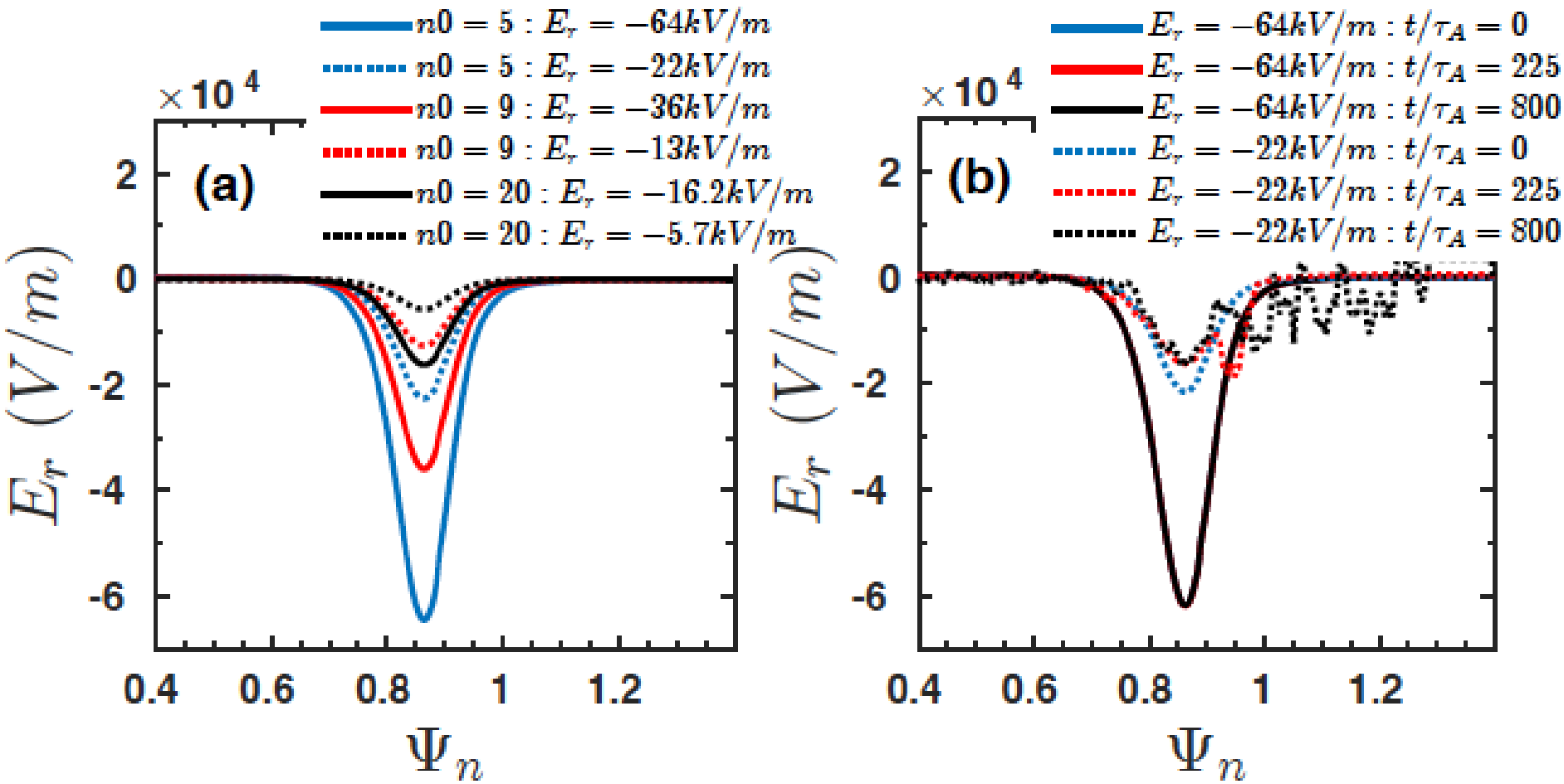

At the beginning, the electric field was increased by a factor of about 3 times

low density, strong current -> peeling dominant, sharp and narrow $\gamma(n)$
high density, weak current -> ballooning dominant, flat and wide $\gamma(n)$

Growth rate spectrums vs density & toroidal mode number

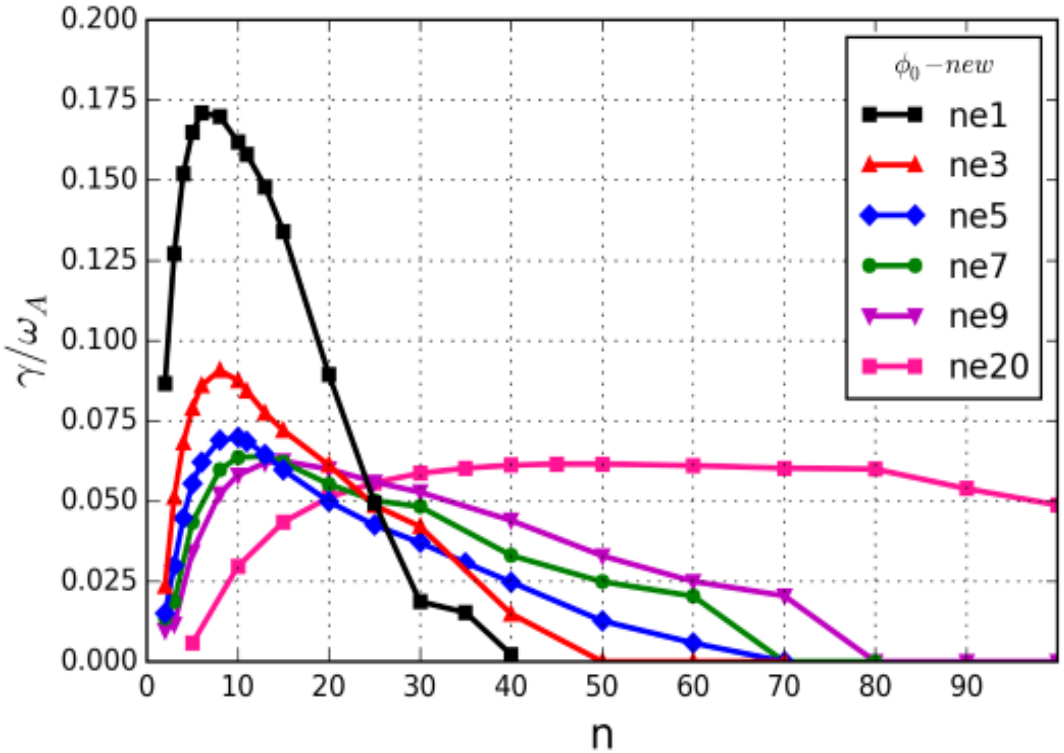

Toroidal mode number

linear growth rate spectrum after turning off peeling drive

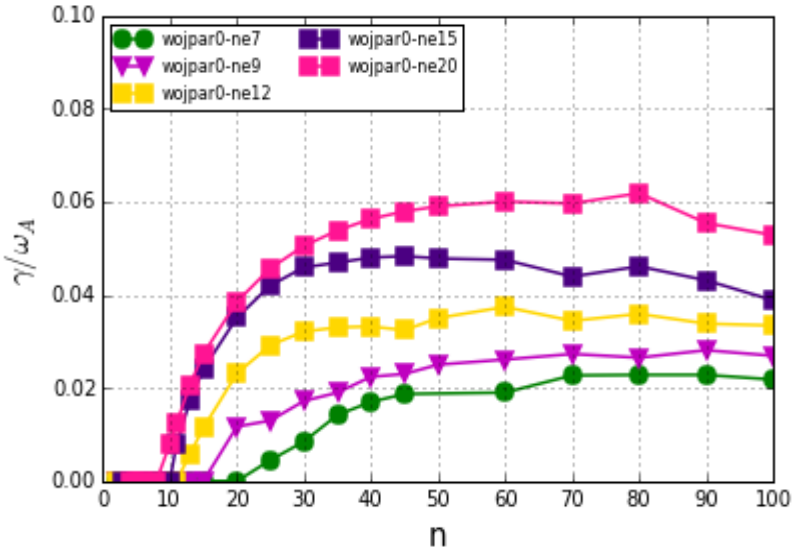

Impact of Er on growth rate of PM, PBM and BM

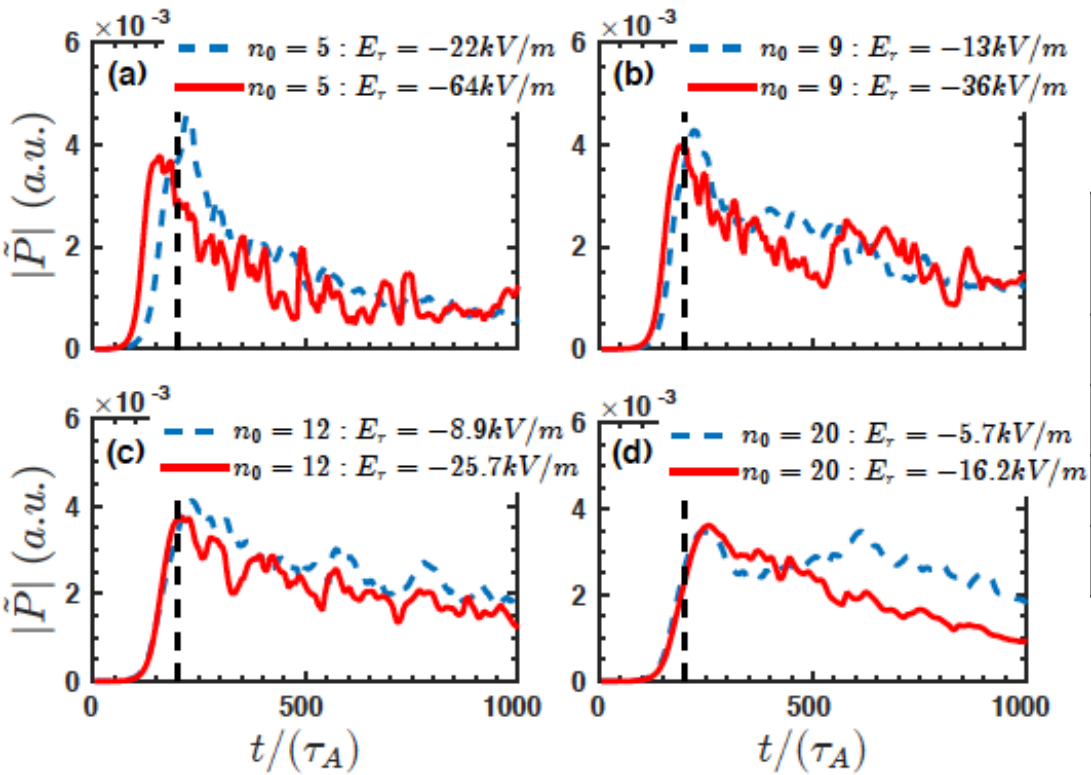

	Growth rate: Er	Growth rate:~3*Er
n0=5: PM	0.058	0.075
n0=9: PM	0.060	0.067
n0=12: PBM	0.062	0.063
n0=20: BM	0.064	0.063

The increase Er only weakly impacts on the amplitude of peeling fluctuations; while the increase Er leads to large suppression of nonlinear ballooning amplitudes.

Increasing Er by a factor of 3, ELM size increases significantly at low collisionality (n_0=5x10^{19} /m^{3}and n_0=9x10^{19}/m^3)

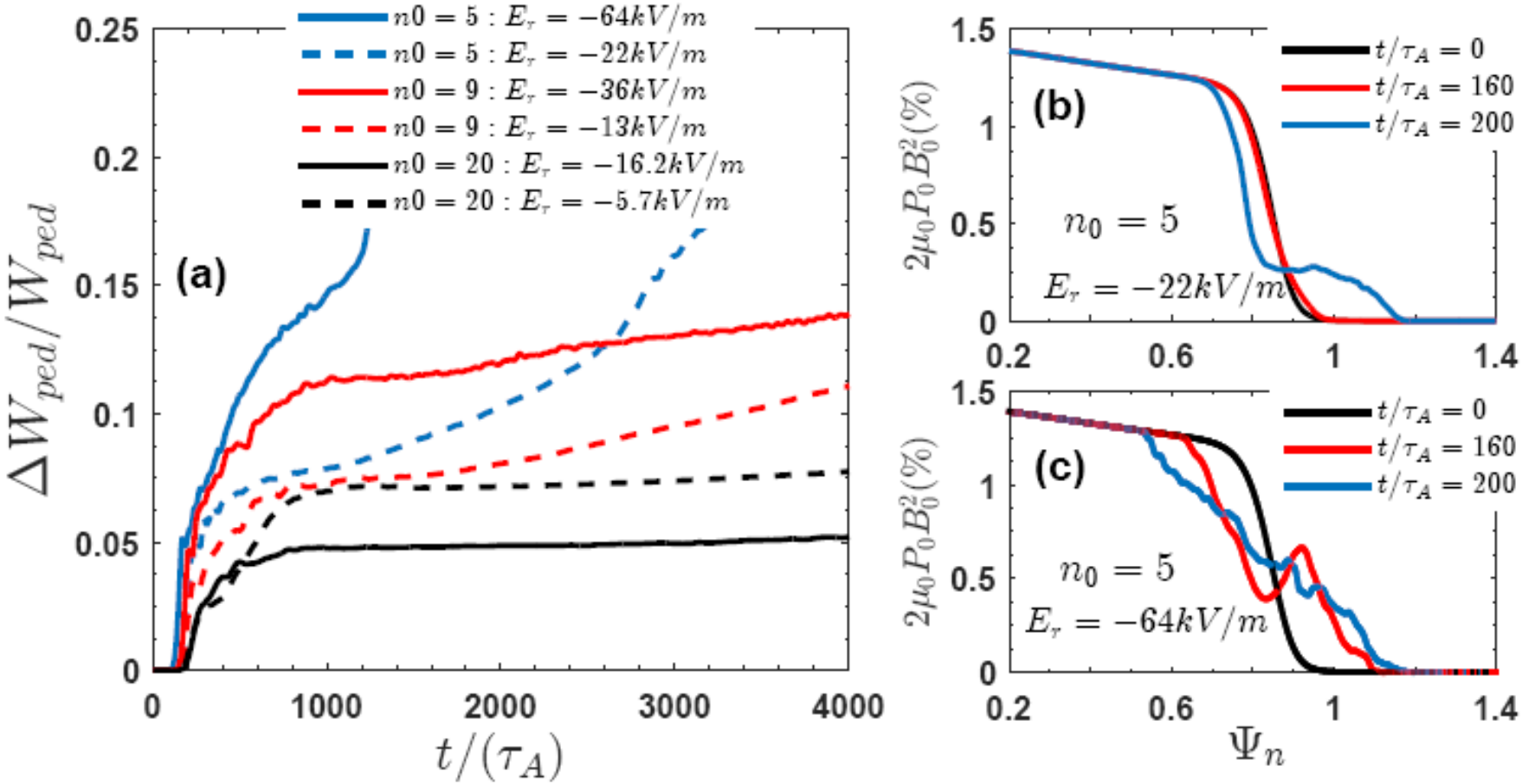

Increasing Er leads to the suppression of ELM size at high collisionality (n_0=20x10^{19}/m^3)

Impact of collisionality and Er on amplitude spectrum and bispectrum of peeling and ballooning mode

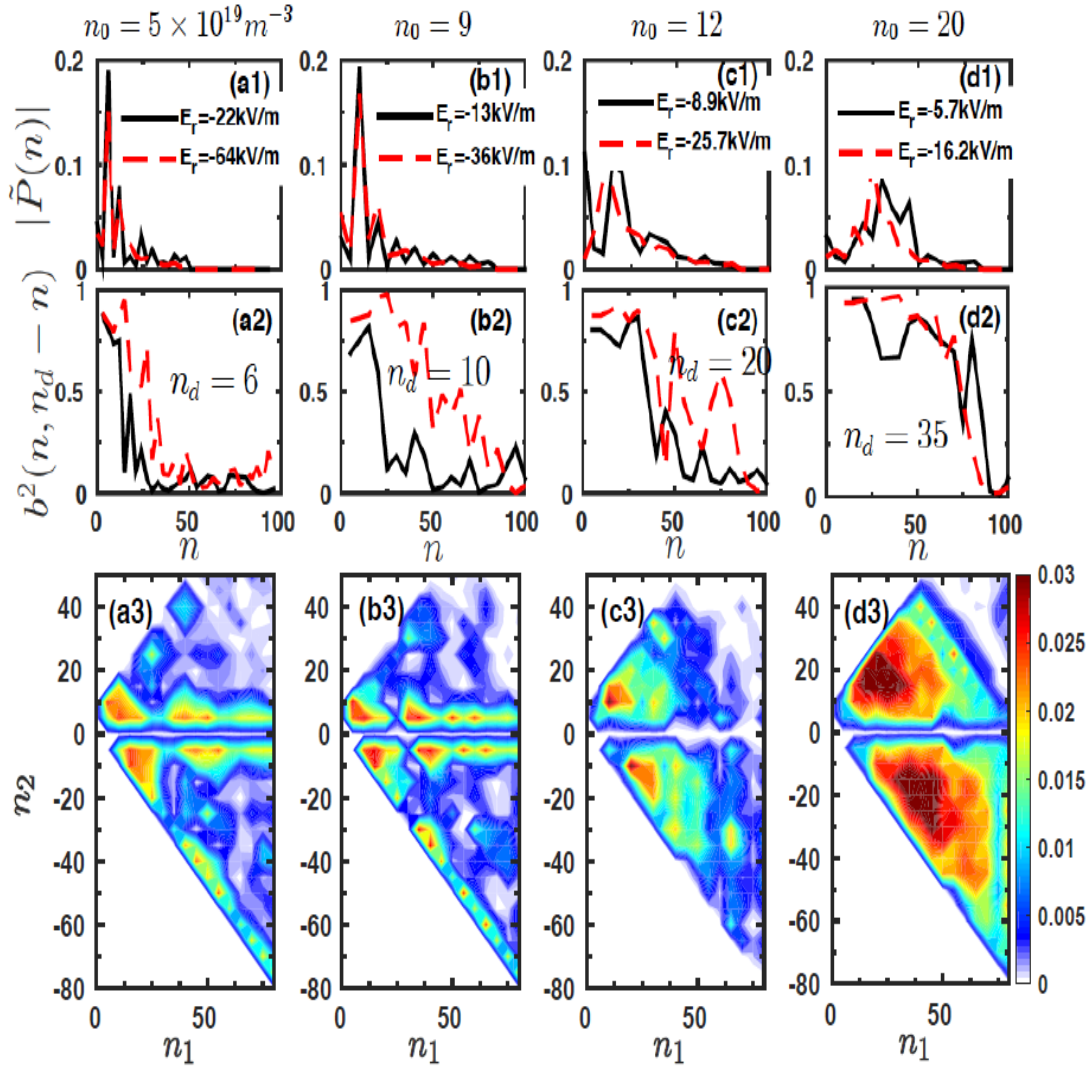

- By increasing collisionality, nonlinear simulations show that
  - amplitude spectrum becomes broad
  - the dominant mode changes from n=6 to n=35
  - nonlinear interactions are strongly enhanced.
- The increase Er can also enhance the nonlinear coupling between modes

ELM suppression by intermittent small scale turbulence induced by SMBI

EAST

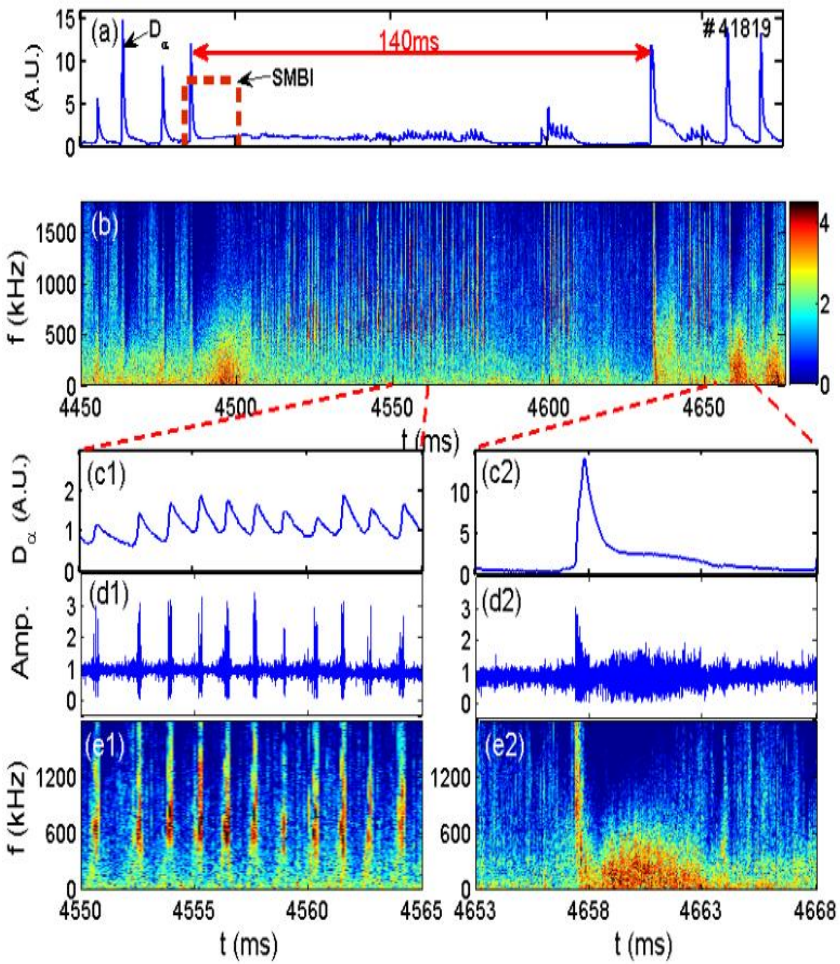

KSTAR

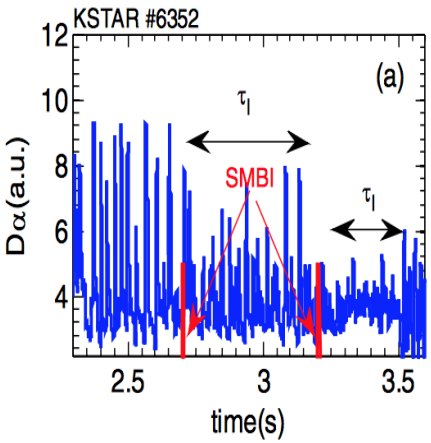

HL-2A

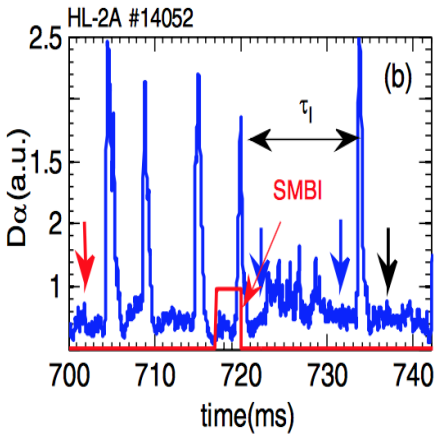

W.W. Xiao NF 54 (2014) 023003

Mitigations of ELM by SMBI have been observed on EAST, KSTAR and HL-2A;

After SMBI

X. L. Zou. 24th IAEA FEC, San Diego, US, (PD/P8-08), 2012.

Experimental results on EAST: Impact of collisionality (with SMBI) on ELM size

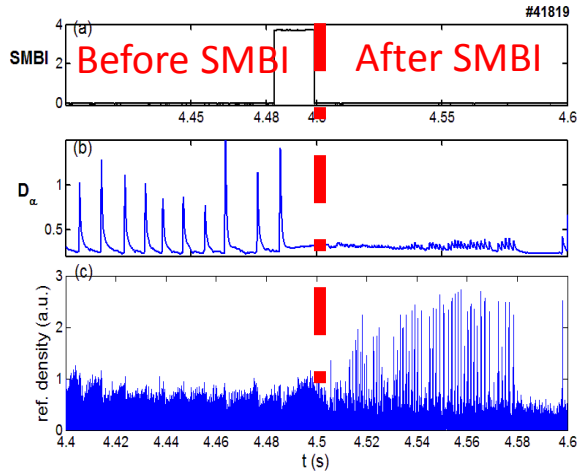

After SMBI (collisionality increased):

1. ELM size is mitigated and particle transport is mainly contributed by high frequency turbulence;
2. Bispectrum analysis indicate that the nonlinear interactions are greatly enhanced at high collisionality.

1. X. L. Zou. 24th IAEA FEC, San Diego, US, (PD/P8-08), 2012.
2. Bispectrum analysis results are provided by Adi Liu (USTC)

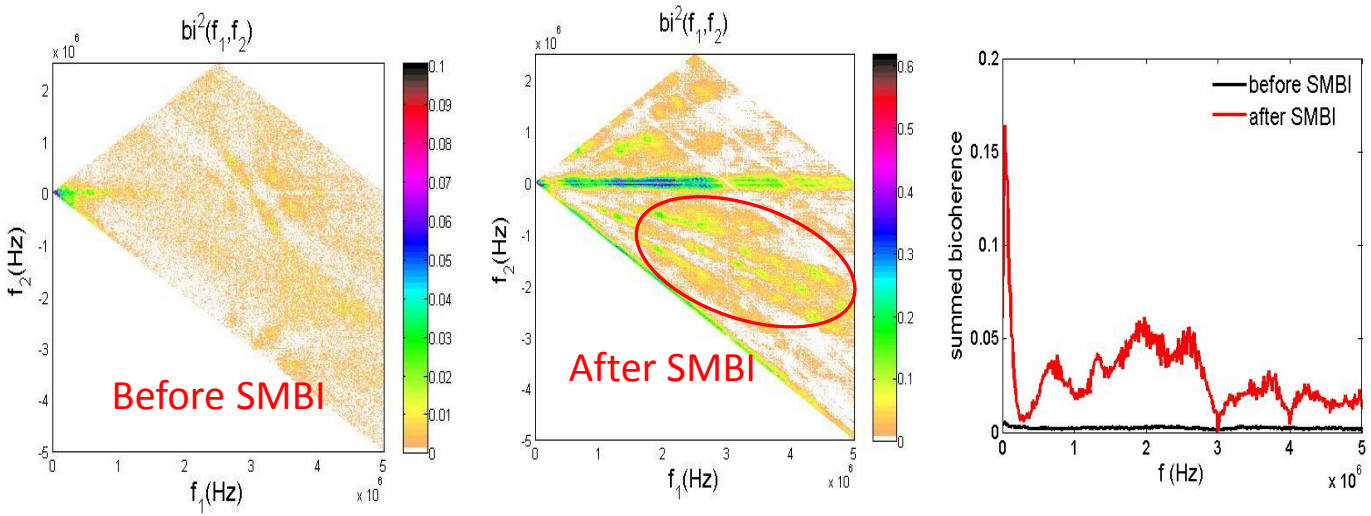

Preliminary experimental results on EAST: Impact of toroidal rotation (Er?) on ELM size

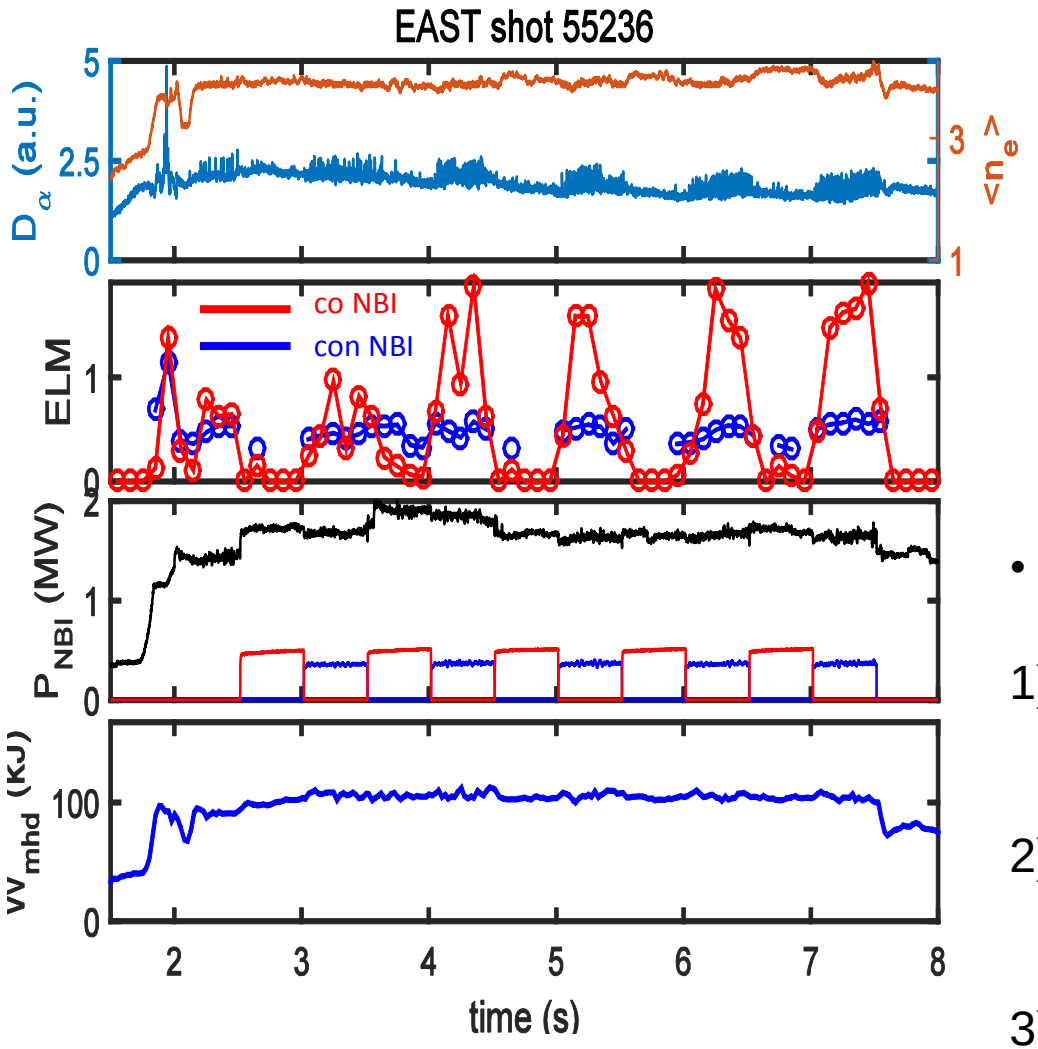

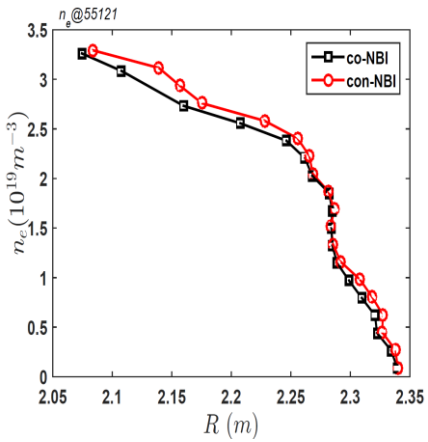

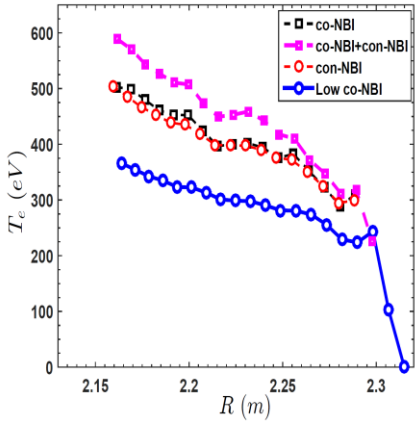

- ELM study with co NBI and con NBI:

1) ELM size is modulated by injecting direction of NBI with smaller ELM size at con NBI.
2) Stored energy and density profiles remain almost the same (collisionality remains the same?)
3) Toroidal rotation (Er) playing an important role in modifying the ELM?

Provided by C.B. Huang (ASIPP)

Impact of co-NBI and con-NBI on nonlinear coupling on EAST

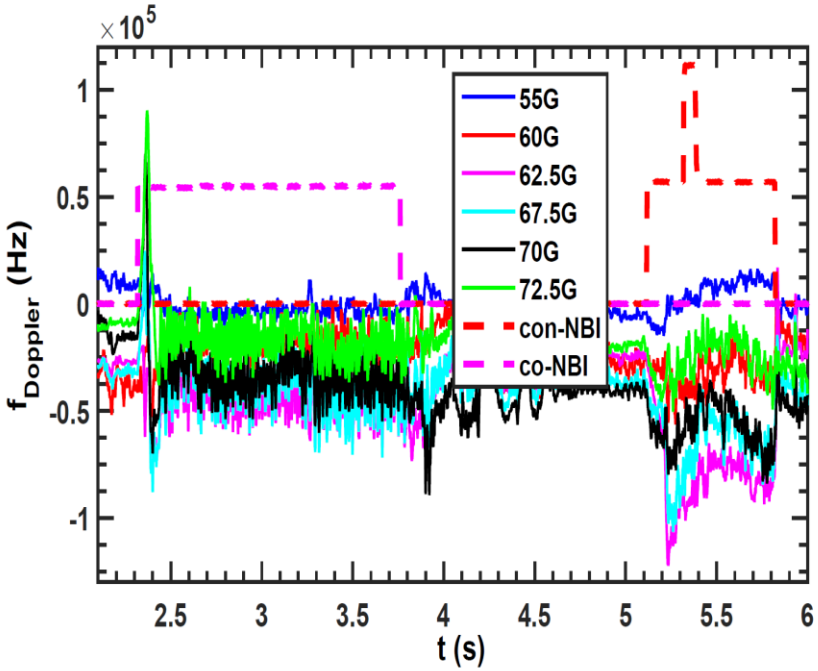

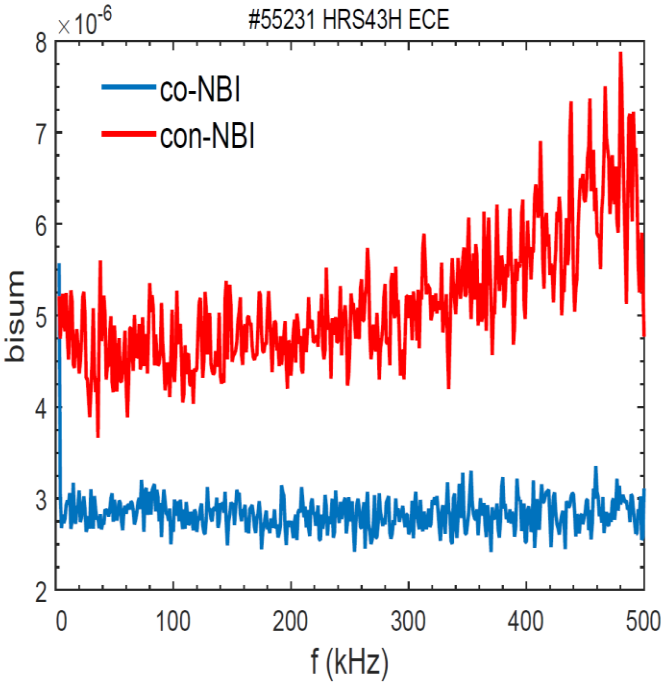

- Left Figure: the electric field ($E_r \propto f_{Doppler}$) with con-NBI is larger than that with co-NBI;
- Right Figure: nonlinear interactions among different modes become stronger in con-NBI (or larger Er) case comparing to the co-NBI case.

- Those observations on EAST are consistent with the simulation results by BOUT++ mentioned before.

Principal Results

- Demonstrated the linear and nonlinear characteristics of ELMs at different collisionality & Er via a density scan

- By increasing collisionality, nonlinear simulations show that
  - ✓ Power spectrum becomes broad, the dominant mode increases from n=6 to n=35
  - ✓ Bispectrum analysis shows that nonlinear mode coupling becomes stronger, resulting in the lack of dominant filamentary structures and reduced ELM energy loss.

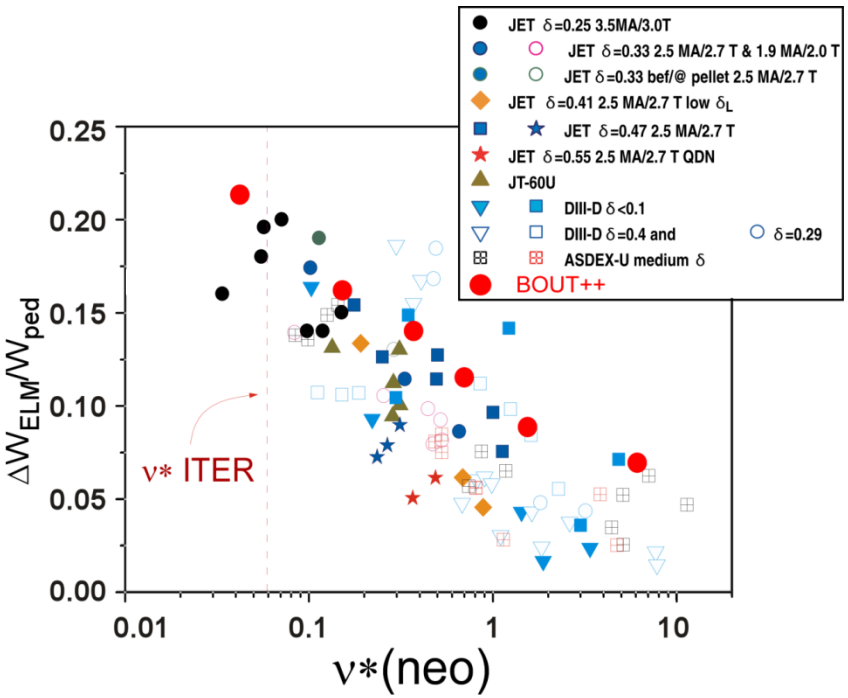

- The impact of radial electric field Er on peeling and ballooning modes is different.
  - ✓ The increase Er significantly enhances the linear growth rate of low-n peeling modes, but only weakly impacts on nonlinear ELM energy loss
  - ✓ The increase Er leads to large suppression of nonlinear ballooning amplitudes, but only weakly impacts on their linear growth rates.

- **New ELM control tool: via radial electric field Er**

Integrated multi-scale simulations for ELM crashes and recovery

Principal results for full ELM cycles with ELM dynamics

- **Separate the dynamical equations into equations for the fluctuating and axisymmetric components to improve computational efficiency**
- **The axisymmetric components of the pressure and vorticity are on the slow transport timescale while the fluctuations are on a rapid timescale to changes in the profiles**
- **The axisymmetric projection of nonlinear fluxes that are bilinear in fluctuating quantities, such as, the energy flux, act as drive terms for the axisymmetric quantities that determine the profiles**

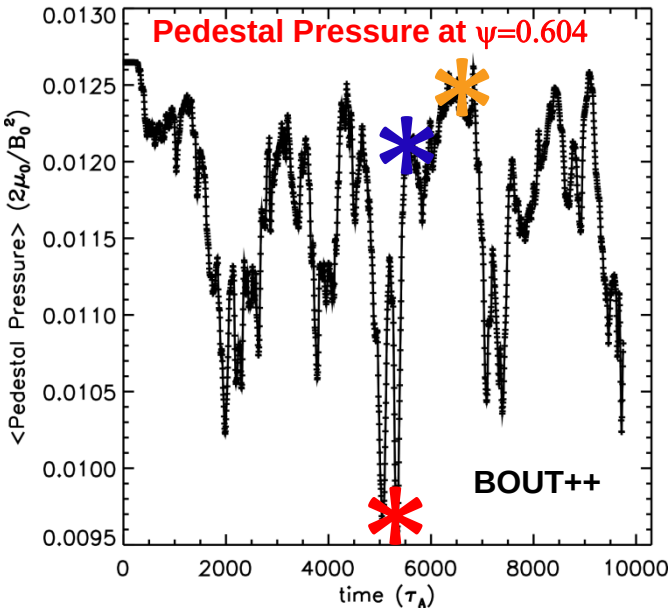

- **The equations are a set of coupled convection-diffusion equations, including**
  - **ELMs**
  - **Micro-turbulence & neoclassical transport**
  - **flux-limited parallel transport**
  - **sources and sinks**

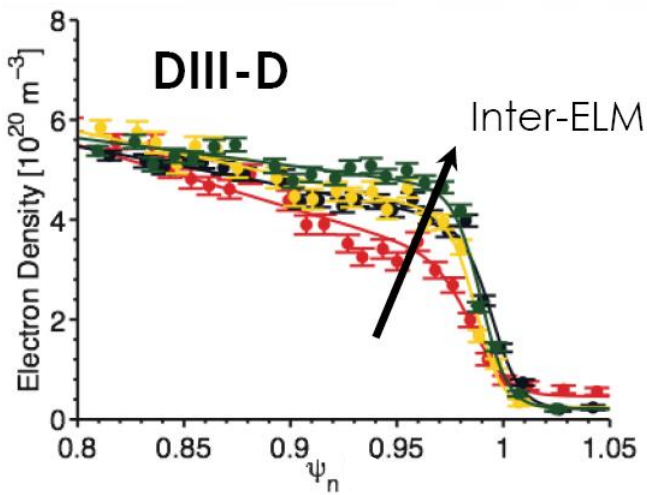

A. Diallo, et al, Phys. Plasmas 22, 056111 (2015)

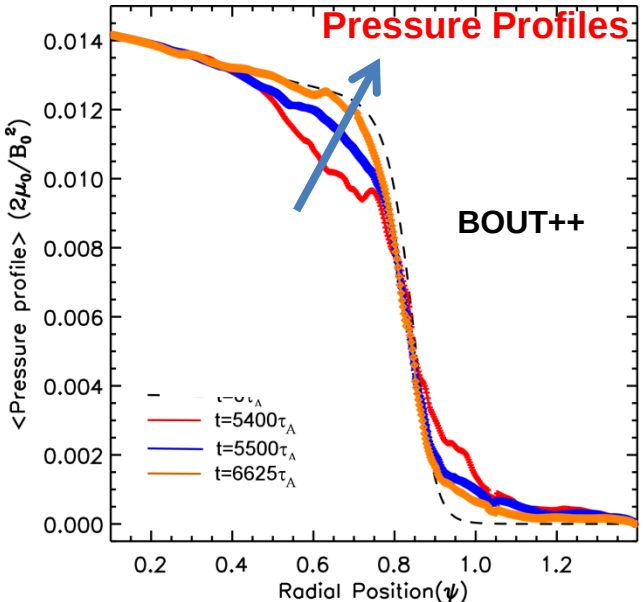

Simulation tracks five ELM cycles for 10000 Alfven times

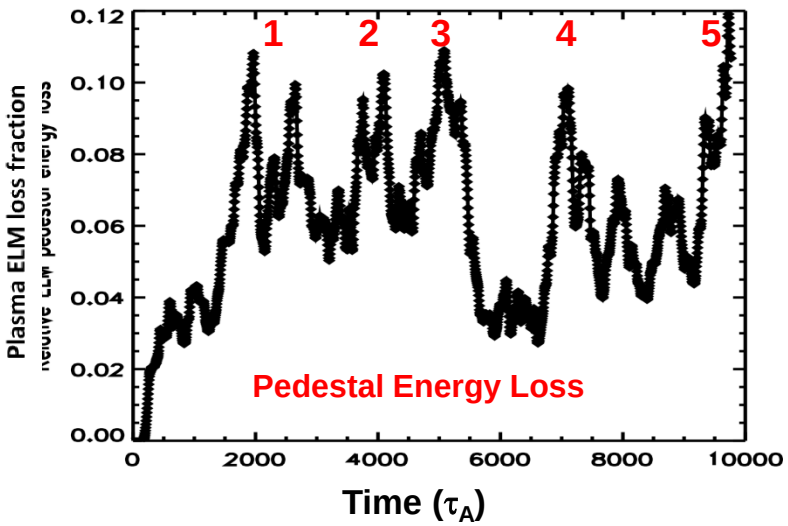

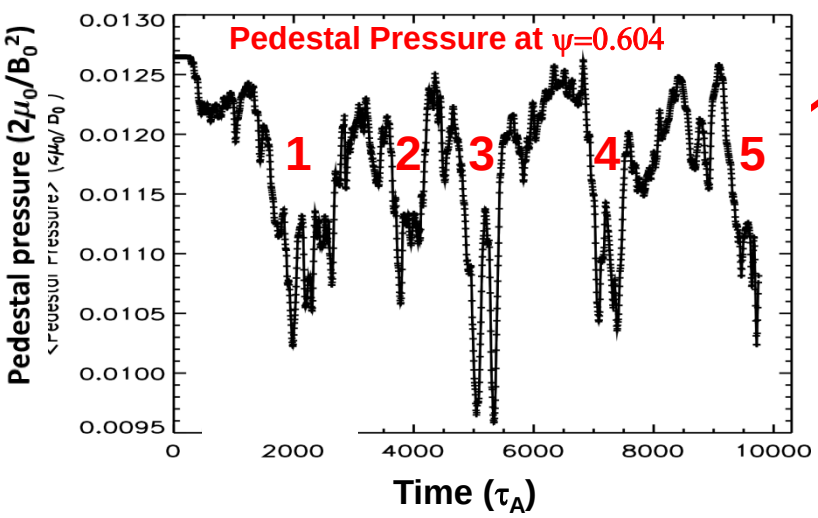

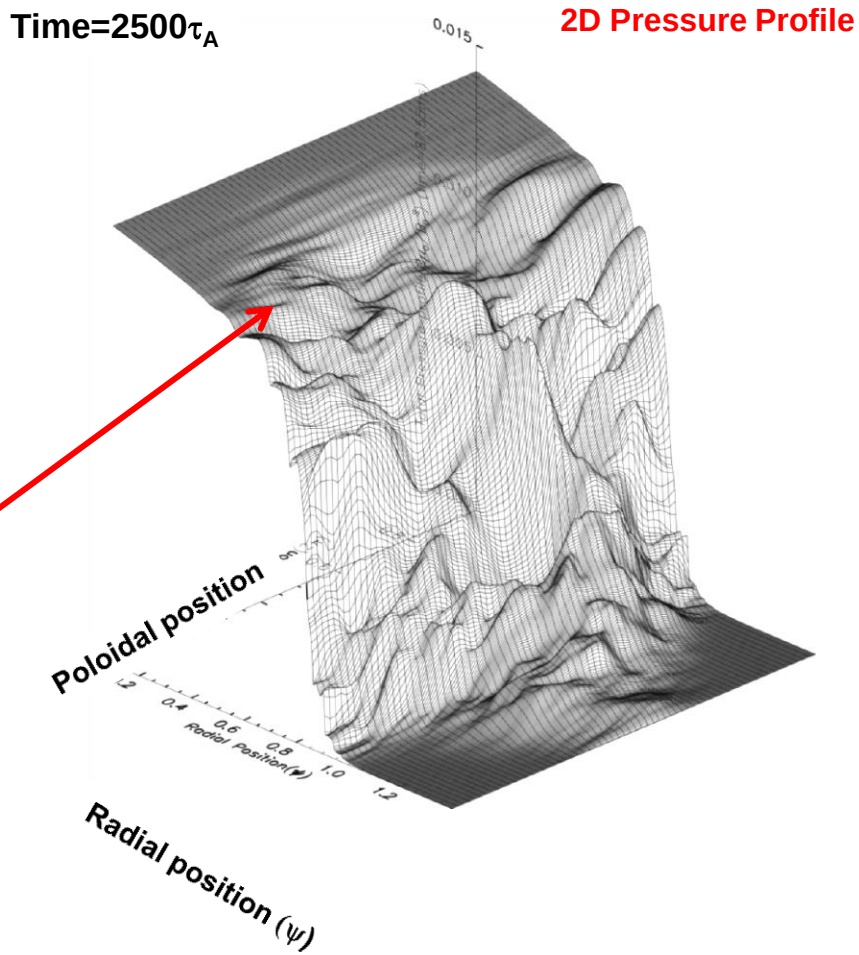

- The pedestal pressure profile collapses and recovers to a steep gradient
- Strong poloidal non-uniformity, even with the flux-limited Spitzer-Harm parallel heat diffusivity

Simulated ELM cycles are similar to DIII-D expts.

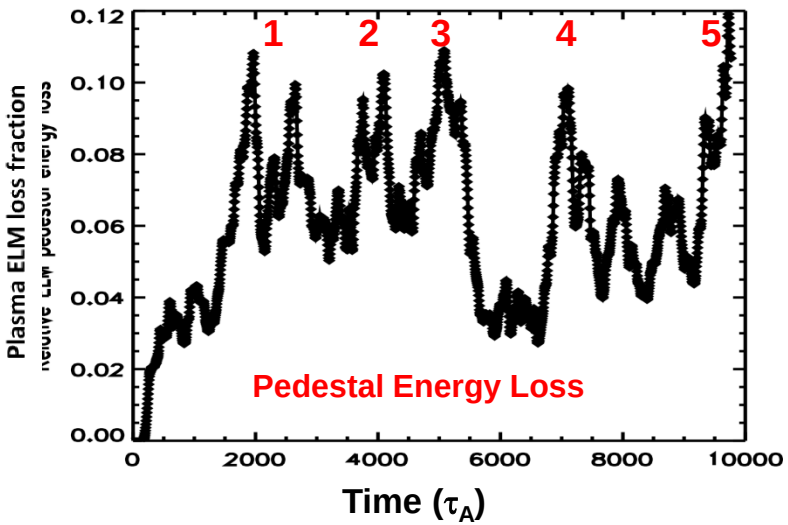

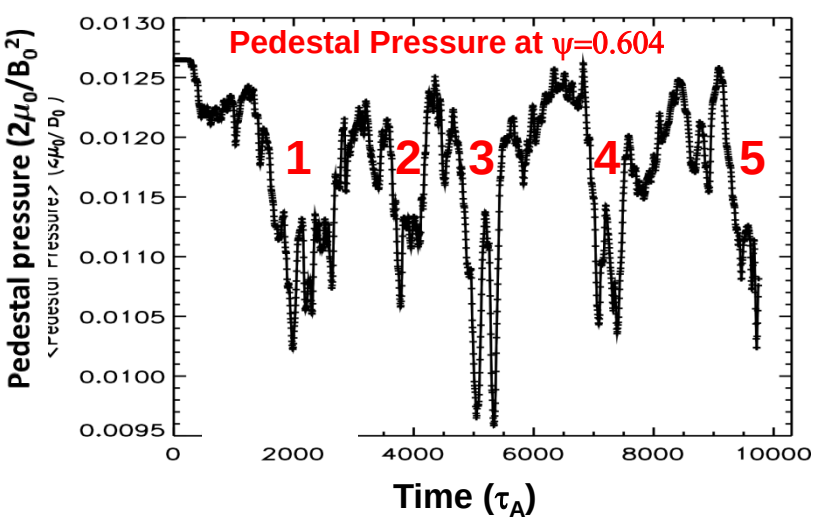

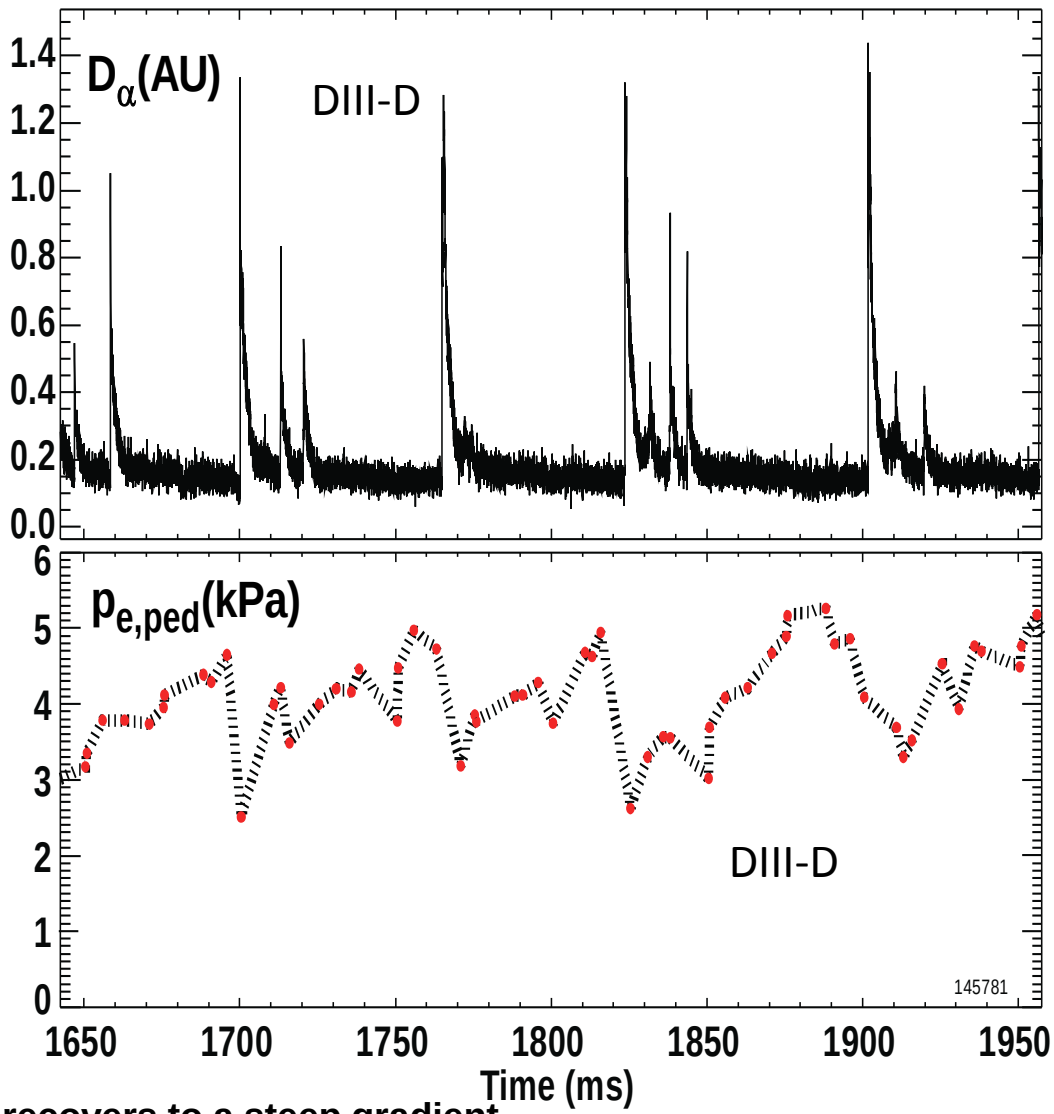

- The pedestal pressure profile collapses and recovers to a steep gradient
- Simulations are for small ELMs, DIII-D data for large ELMs

In addition to ELMs,

Fluctuations are simulated for comparison Between ELMs in H-mode & During ELM-suppressed I-Modes

(module 6f_divertor_imp)

- **BOUT++ 3D 6-field 2-fluid electromagnetic model evolves**
  - ✓ **density n_i,**
  - ✓ **ion temperature T_i**
  - ✓ **parallel velocity $v_{||i}$**
  - ✓ **electron temperature T_e**
  - ✓ **vorticity ϖ**
  - ✓ **magnetic vector potential $A_{||}$**
- **Based on a set of C-Mod and DIII-D experiments**
  - ✓ **realistic X-point magnetic and plasma profiles**
  - ✓ **BOUT++ computation region across the magnetic separatrix**

Various coherent fluctuation structures observed in Alcator C-Mod and other Tokamaks

I-modes: has a temperature pedestal but no density pedestal , ELM-free

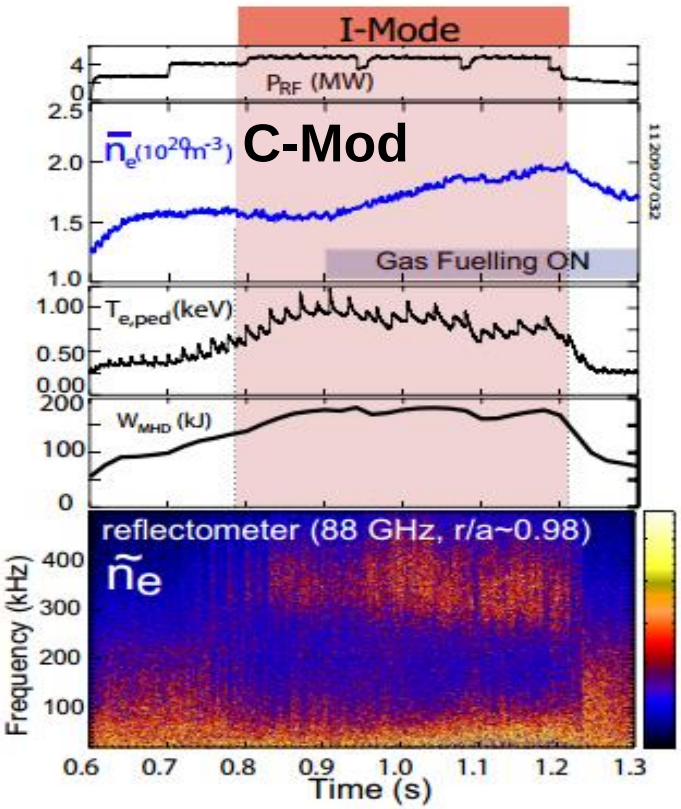

A Hubbard
2015 APS Invited KI2.03
2012 IAEA EX/1-3

I.Cziegler
2015 APS Invited BI2.04

- **Weakly Coherent Modes (WCMs) in I-mode**
  - ✓ **mid-range frequency,(~200-400 kHz)**
  - ✓ **lead to large D_e, $D_e > \chi_e$**

ELMy H-mode on C-Mod

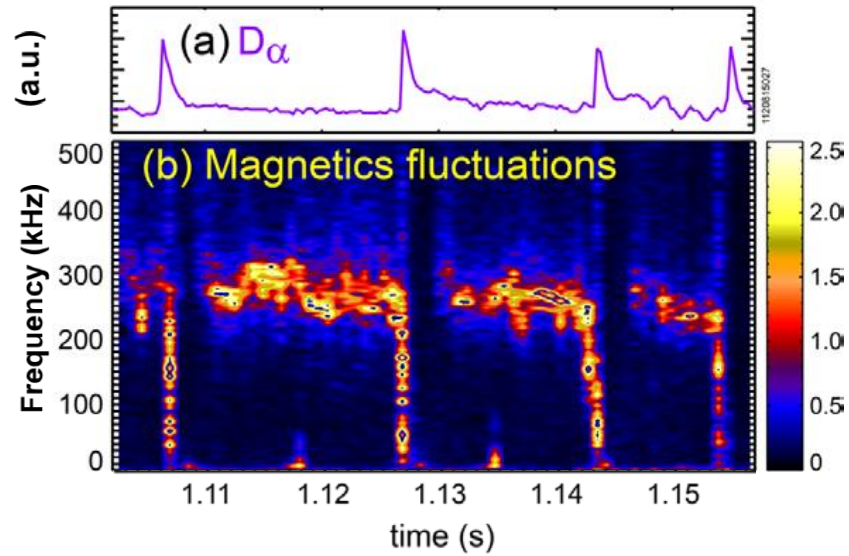

J. W. Hughes, Nucl. Fusion 53 (2013) 043016
A Diallo, APS invited, 2014,
A Diallo, PRL v112 115001(2014)

JET-Perez PPCF 2004
AUG-Laggner EPS 2015

- **There is experimental evidence that Quasi-coherent fluctuations (QCFs) lead to the saturation of the pedestal between ELMs on C-Mod, DIII-D, AUG, & JET**
  - ✓ **QCFs Observed as density & magnetic fluctuations**
  - ✓ **Pedestal-Localized QCFs with onsets for ∇T_e**
- **QCFs are different from QCMs in ELM-free EDA H-mode**

C-Mod experimental plasma profiles are used in Kinetic EFIT MHD equilibria calculations and BOUT++ simulations

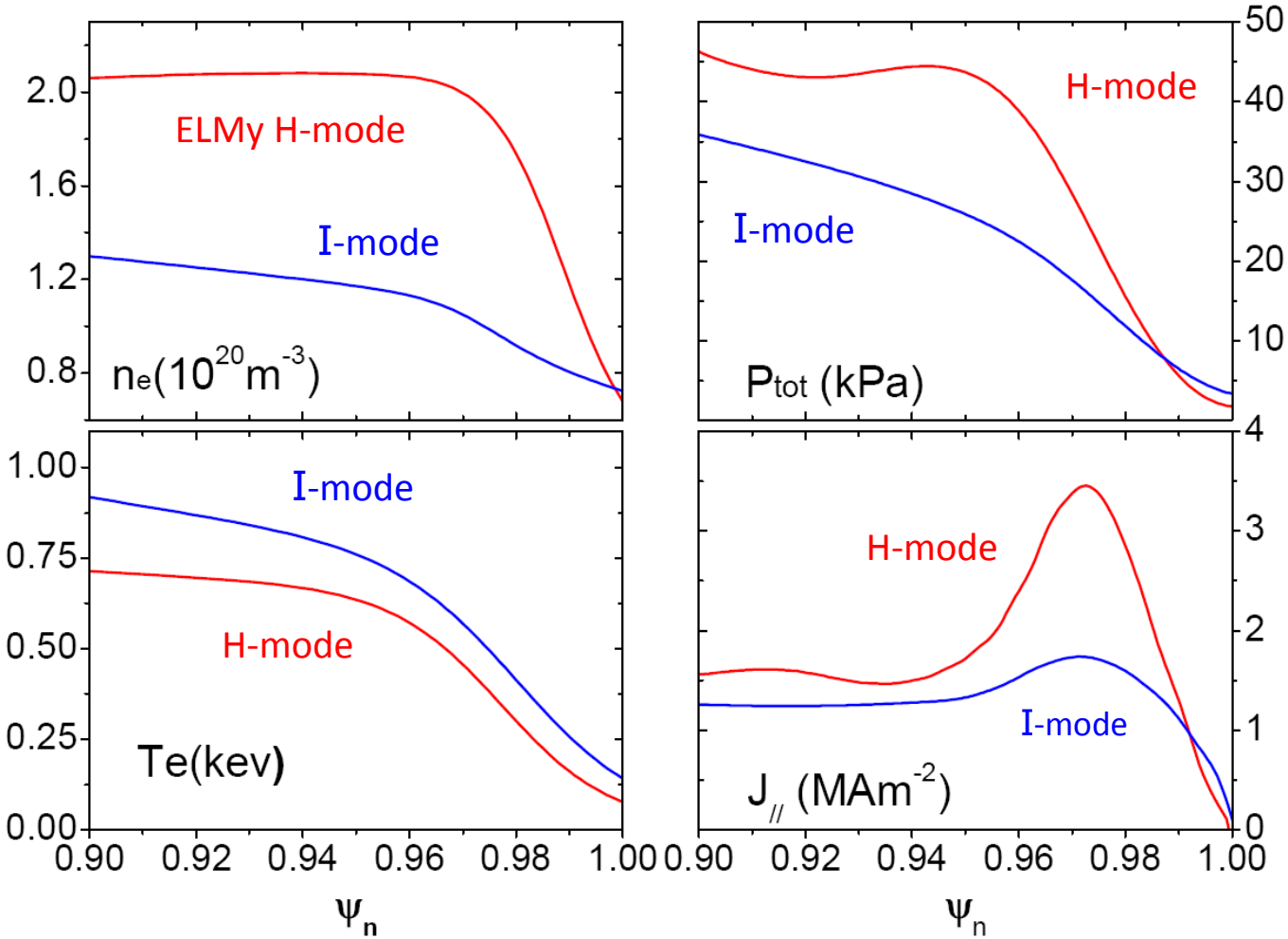

I-mode: 1120907032@1010ms

H-mode: 1120815027@1075ms

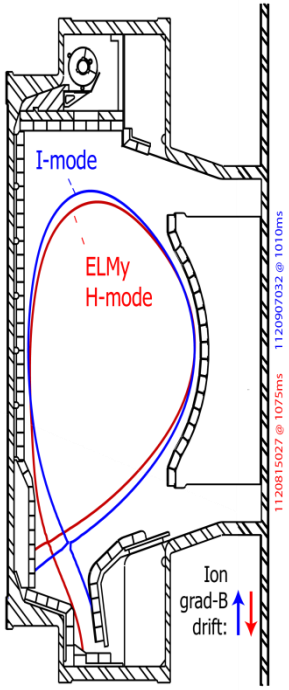

- **Dedicated ELMy discharges were performed**
  - **B_T = 5.4 T & Ip =0.9 MA**
- **Difference between the I-mode and H-mode pedestals**
  - **Lack of a particle barrier & no ELMs in I-mode**

- **I-mode has lower pressure & current than H-mode**
  - **Weakly Coherent Modes (WCMs) in I-mode**
  - **Quasi-coherent fluctuations (QCFs) between ELMs in ELMy H-mode**

C-Mod pedestal simulations show ELMy H-mode and I-mode exhibit different underlying instabilities

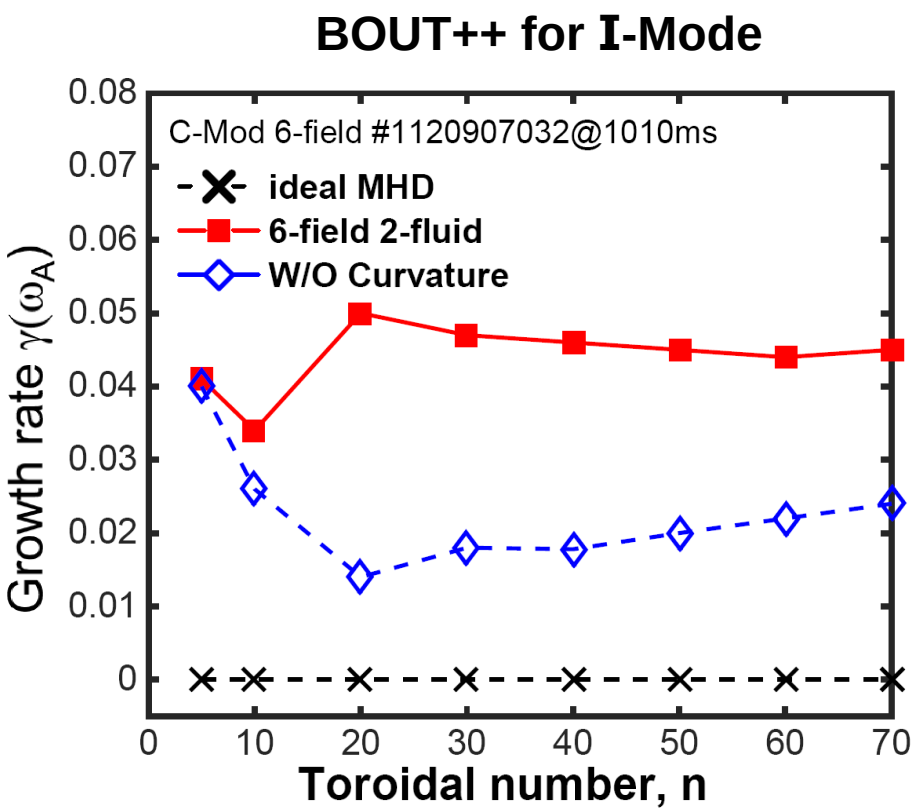

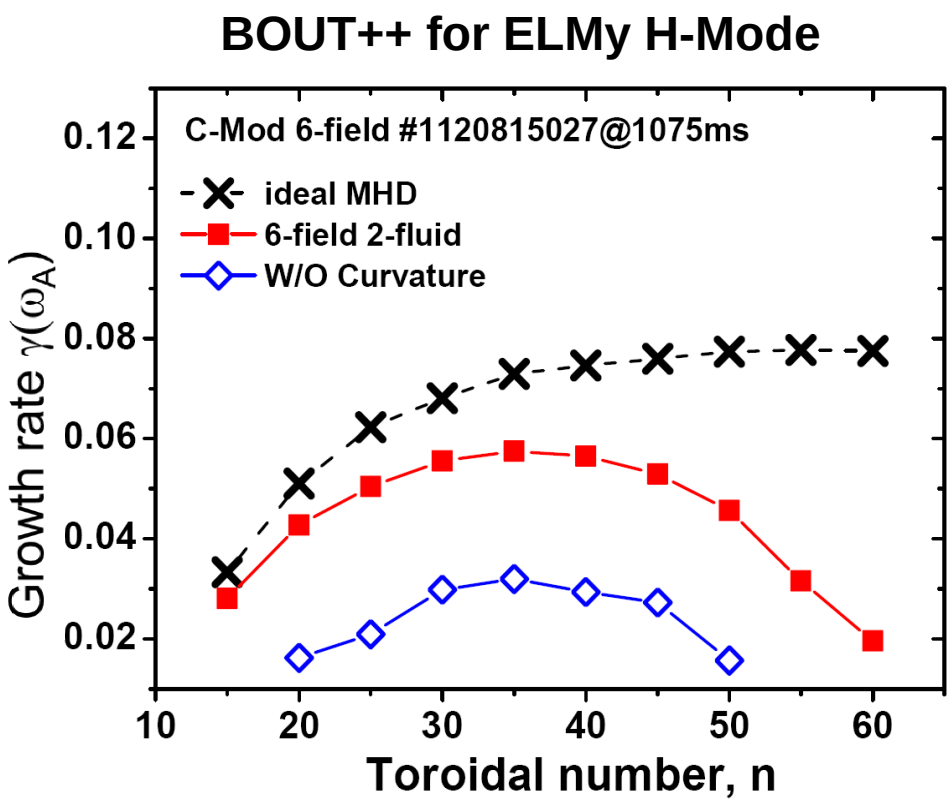

Linear simulations indicate that

- **WCMs are unstable for resistive ballooning mode and drift-Alfven wave**
- **QCFs are marginal unstable near Peeling-Ballooning threshold**

BOUT++ simulations show similar evolution of Quasi-Coherent Fluctuations as C-Mod magnetic probe measurements and good agreement

- ✓ Pedestal-Localized QCFs
- ✓ $k_\theta \sim 0.7\ cm^{-1}$, toroidal mode number n~10
- ✓ f ~ 300-400kHz

BOUT++

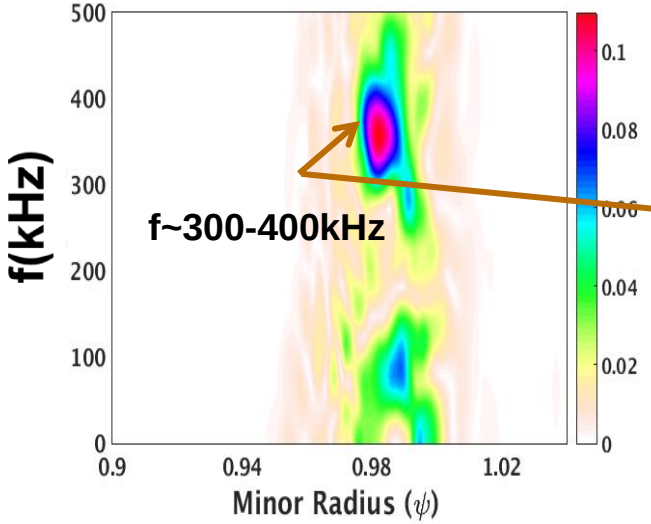

C-Mod

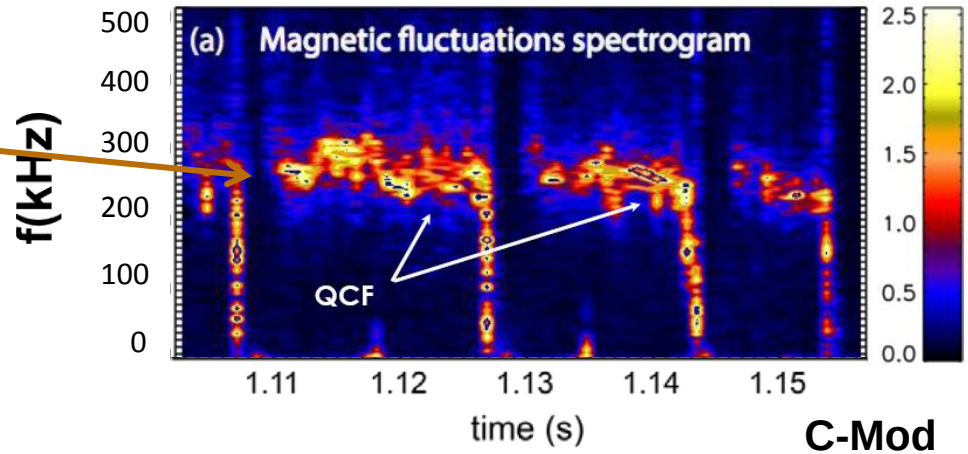

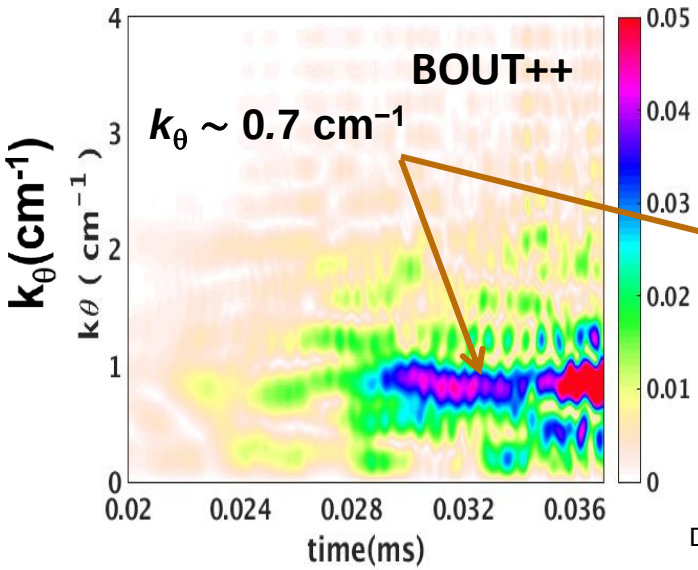

C-Mod

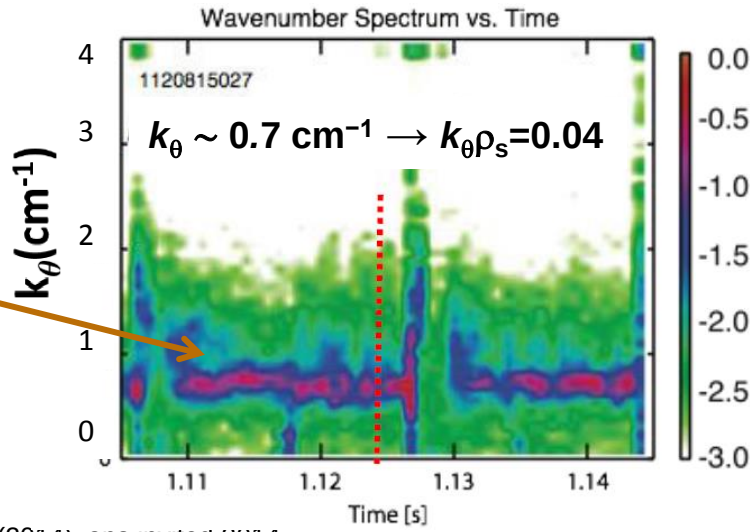

Diallo, PRL 112, 115001 (2014), aps invited 2014

Linear and nonlinear BOUT++ analyses show similar frequency evolution as Quasi-Coherent Fluctuations (QCFs) on DIII-D expts.

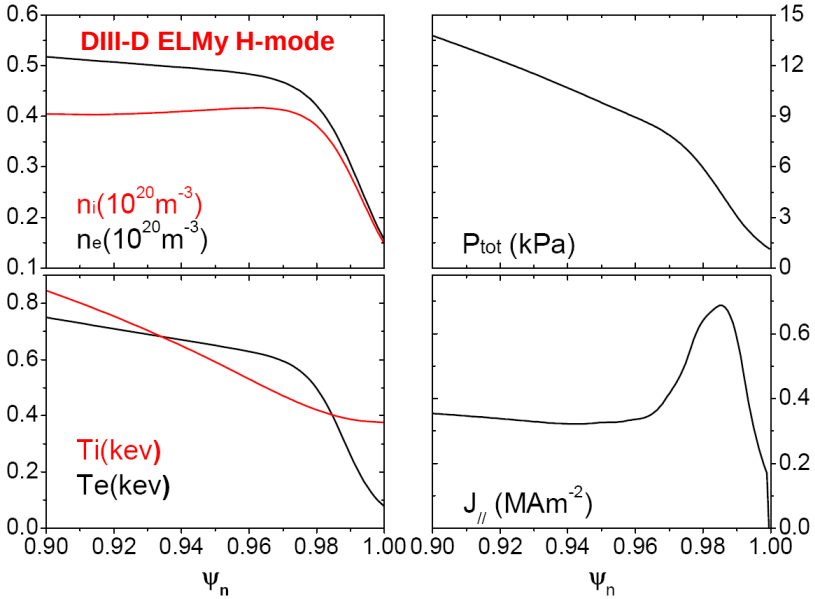

- Normal B_T =1.9 T with q_{95} = 3 in Type I ELMy H-mode
- Linear analysis indicates:
  - ✓ edge is marginally unstable for ballooning modes
  - ✓ n=40 is the most unstable when diamagnetic effects are included
  - ✓ drift Alfven mode appears to be dominant
- Nonlinear analysis indicates
  - ✓ The frequency of the dominant mode is approx. 80 kHz which is near that of observed QCFs

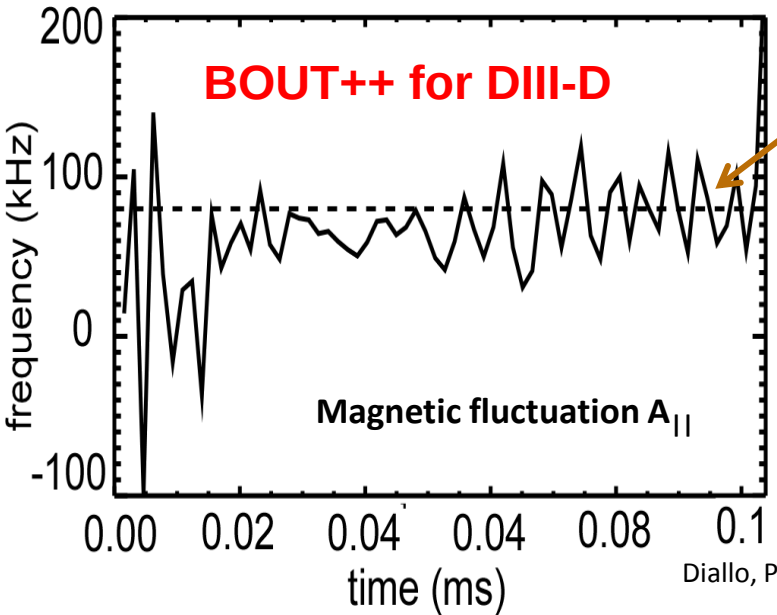

QCF
f~80kHz

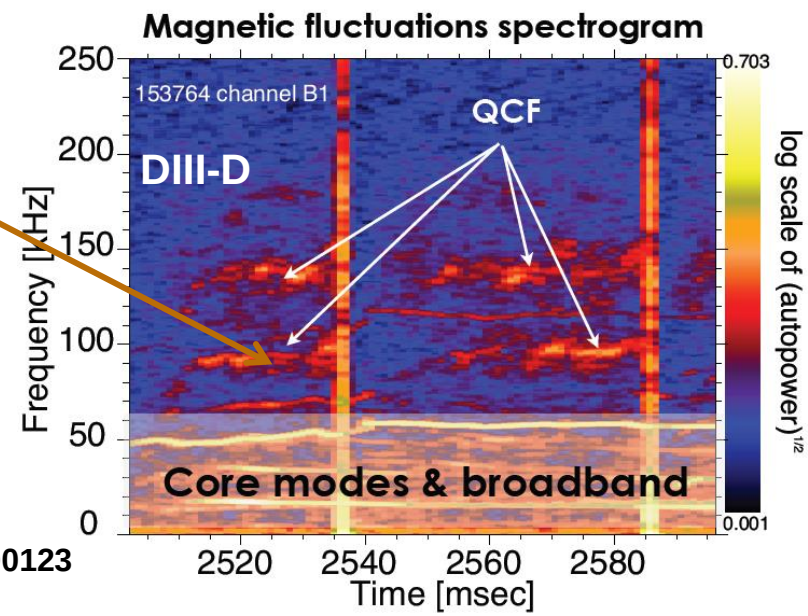

T. Y. Xia TP12.00123

Diallo, Phys. Plasmas 22, 056111 (2015)

BOUT++ simulations of C-Mod show similar onsets of the QCF with electron temperature gradient ∇T_e observed in DIII-D

DIII-D expt.

Diallo, Phys. Plasmas 22, 056111 (2015)

Evolution of QCF amplitude and Temperature gradient

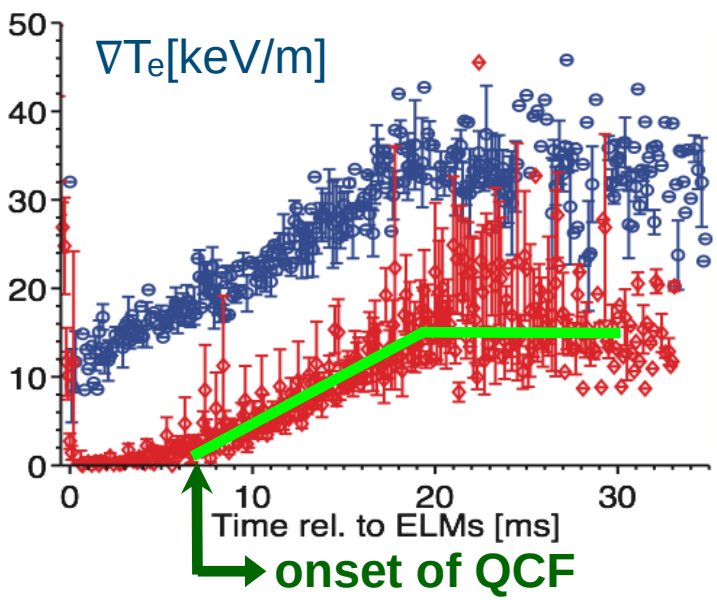

BOUT++ for C-Mod

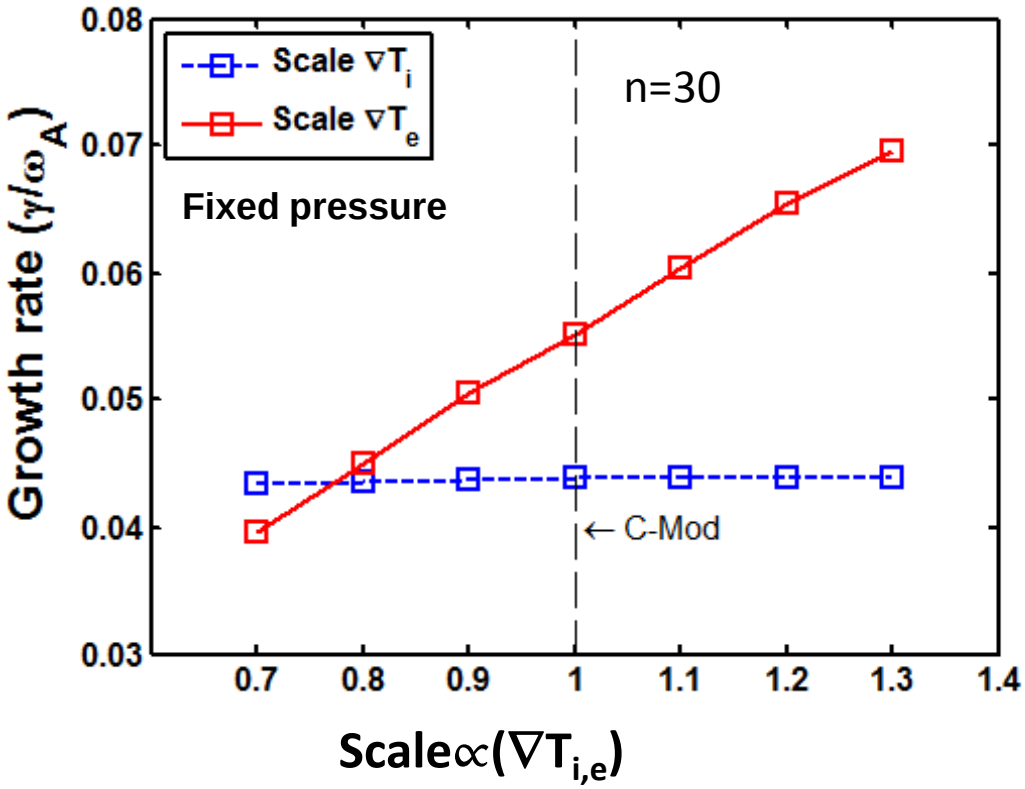

- **QCF onsets for a given critical temperature gradient ∇T_e**
- **Temperature gradient ∇T_e and QCF amplitude track each other**

Increasing ∇T_e at the edge should increase the QCFs intensity, while increasing ∇T_i doesn't.

Weakly Coherent Modes (WCMs) in I-modes have been simulated for comparison with expts.

The dominant mode n=20 near the position of the reflectometer shows a similar frequency peak in I-Modes

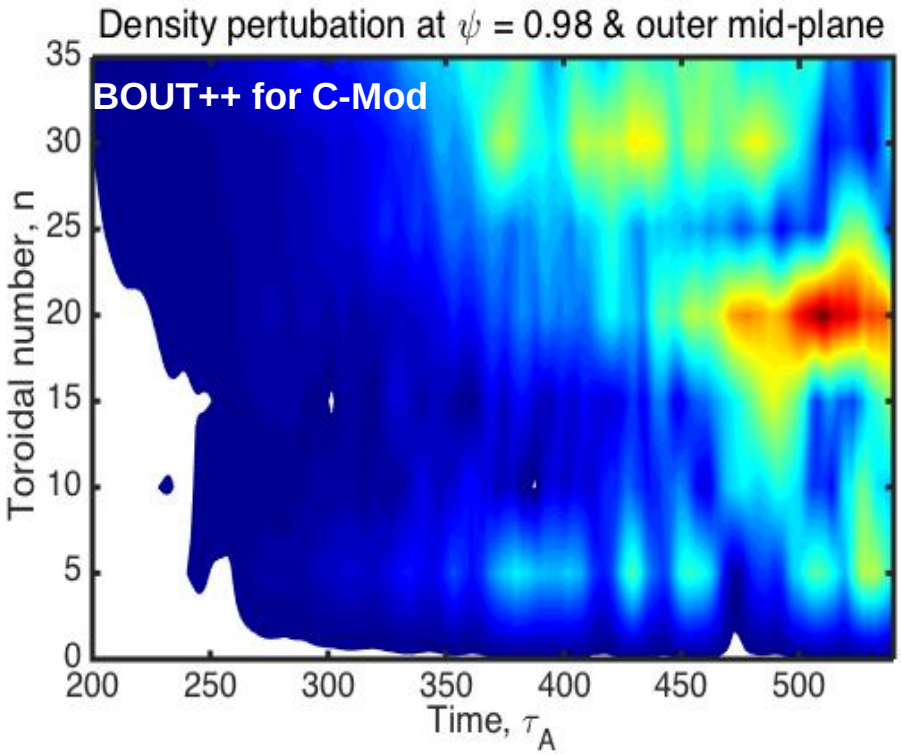

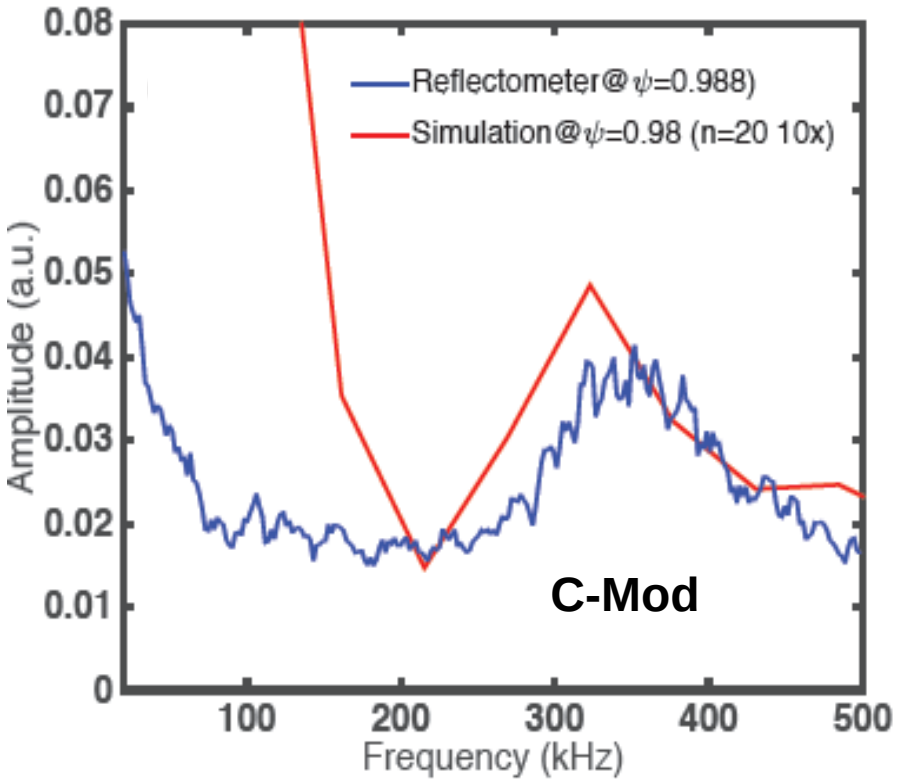

- **The spectrum of the mode n=20 is similar to the experimental result from the reflectometer**
- **The spectrum of total modes also has the peak around 300kHz.**

Z. X. Liu et al, GO4.00005, Analysis of Weakly Coherent mode on C-Mod with the BOUT++ code, 10:18AM - 10:30AM, Tuesday, November 17, 2015, in session of C-Mod, ADX, Lockheed Martin CFR

I-mode: **Particle diffusivity is larger than thermal ($D >> \chi_e$)**
H-mode: **Particle diffusivity is smaller than thermal ($D << \chi_e$)**

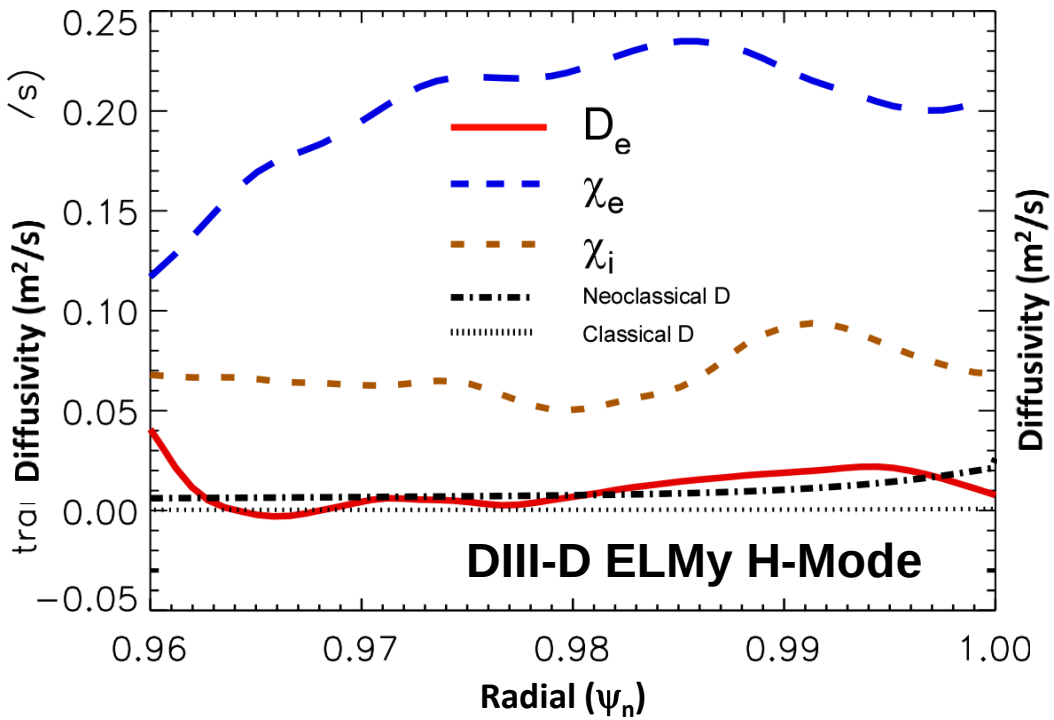

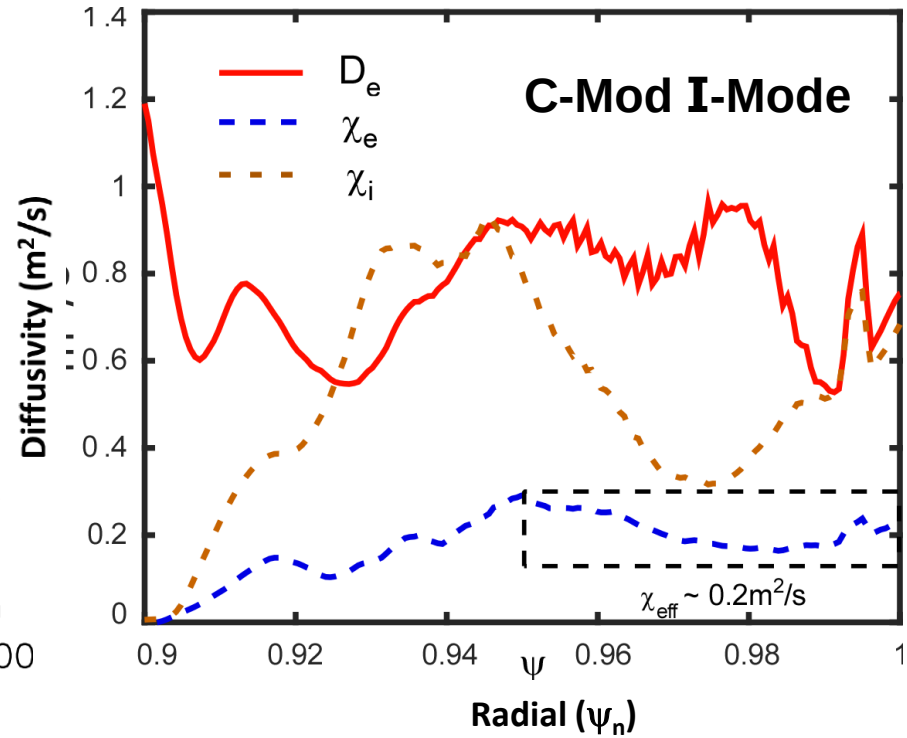

- **Larger particle diffusivity is consistent with the key feature of I- mode, $D >> \chi_e$**
- **Predicted χ_e and χ_i (dashed curves) are close to experimental χ_{eff} (from power balance over $0.95 < \psi < 1$) for I-mode**

Summary

The high-fidelity BOUT++ two-fluid suites have demonstrated significant recent progress toward integrated multi-scale simulations

- ✓ **including ELM dynamics, evolution of ELM cycles, and continuous fluctuations, as expts.**

- **Nonlinear ELM simulations show three stages of an ELM event**
  - ✓ **Collisionality scaling of ELM energy losses consistent with ITPA multi-tokamak database**

- **Nonlinear integrated multi-scale ELM simulations:**
  - ✓ **Simulation tracks five ELM cycles for 10000 Alfven times for small ELMs**

- **To validate BOUT++ simulations & find better regimes, both quasi-coherent fluctuations (QCFs) in ELMy H-modes and Weakly Coherent Modes (WCMs) in I-modes have been simulated for comparison with expts.**
  1) **H-mode simulations predict that**
     - ✓ **the QCFs are near marginal instability for ideal peeling-ballooning modes**
     - ✓ **the predicted particle diffusivity is smaller than the heat diffusivity, $D \gg \chi_e$**
  2) **I-mode simulation results are that**
     - ✓ **a strong instability exists at $n \geq 20$, for resistive ballooning modes and drift-Alfven wave**
     - ✓ **the predicted particle diffusivity is larger than the heat diffusivity, $D \ll \chi_e$**

- **A successful cooperation between simulation and experiment teams**